TECHNICAL REPORT ARSCD-CR-8001

FINE GRAIN ALUMINUM SUPERPLASTICITY

C. H. HAMILTON

FEBRUARY 1980

US ARMY ARMAMENT RESEARCH AND DEVELOPMENT COMMAND
FIRE CONTROL AND SMALL CALIBER
WEAPON SYSTEMS LABORATORY
DOVER, NEW JERSEY

The citation in this report of the names of commercial firms or commercially available products or services does not constitute official endorsement or approval of such commercial firms, products, or services by the U.S. Government.

The views, opinions, and/or findings contained in this report are those of the author and should not be construed as an official Department of the Army position, policy, or decision unless so designated by other documentation.

Unclassified

SECURITY CLASSIFICATION OF THIS PAGE (When Date Entered)

REPORT DOCUMENTATION PAGE

READ INSTRUCTIONS BEFORE COMPLETING FORM

1. REPORT NUMBER: ARSCD-CR-8001
2. GOVT ACCESSION NO.:
3. RECIPIENT'S CATALOG NUMBER:

4. TITLE (and Subtitle): FINE GRAIN ALUMINUM SUPERPLASTICITY

5. TYPE OF REPORT & PERIOD COVERED: Final Report 09/29/78 through 03/31/79

6. PERFORMING ORG. REPORT NUMBER: SC5187.13FR

7. AUTHOR(s): C. H. Hamilton

8. CONTRACT OR GRANT NUMBER(s): DAAK10-78-C-0424

9. PERFORMING ORGANIZATION NAME AND ADDRESS:
Rockwell International Science Center
1049 Camino Dos Rios
Thousand Oaks, California 91360

10. PROGRAM ELEMENT, PROJECT, TASK AREA & WORK UNIT NUMBERS:
DA Project 1L162105AH84
AMCMS Code 612105.11.8400

11. CONTROLLING OFFICE NAME AND ADDRESS:
ARRADCOM, TSD
STINFO (DRDAR-TSS)
Dover, New Jersey 07801

12. REPORT DATE:

13. NUMBER OF PAGES: 63

14. MONITORING AGENCY NAME & ADDRESS (if different from Controlling Office):
ARRADCOM, FC & SCUSL
Materials and Manufacturing Division (DRDAR-SCM-P)
Dover, New Jersey 07801

15. SECURITY CLASS. (of this report): Unclassified

15a. DECLASSIFICATION/DOWNGRADING SCHEDULE:

16. DISTRIBUTION STATEMENT (of this Report):
Approved for public release; distribution unlimited.

17. DISTRIBUTION STATEMENT (of the abstract entered in Block 20, if different from Report):

18. SUPPLEMENTARY NOTES:

19. KEY WORDS (Continue on reverse side if necessary and identify by block number):
Superplastic aluminum, Superplasticity, Superplastic forming, High strength aluminum alloy, 7475 aluminum alloy, Grain growth

20. ABSTRACT (Continue on reverse side if necessary and identify by block number):
Fine grained 7475 aluminum alloy sheet was evaluated for its superplastic properties and potential for superplastic forming. The sheet alloy was specially processed by the ALCOA Technical Laboratory utilizing procedures prescribed by the contractor to achieve a fine grain size. The grain size measurements on this sheet alloy after complete recrystallization revealed a short transverse dimension of 7.8 μm and longitudinal and long transverse dimensions of 14 μm. Subsequent grain growth studies showed that this fine grain size developed is quite stable at temperatures as high as 516°C (960°F).

DD FORM 1 JAN 73 1473 EDITION OF 1 NOV 65 IS OBSOLETE

Unclassified

SECURITY CLASSIFICATION OF THIS PAGE (When Date Entered)

20. ABSTRACT (continued)

High temperature testing was conducted over the temperature range of 427°C (800°F) to 516°C (960°F) in order to establish the strain rate sensitivity of flow stress, strain hardening characteristics, and total elongation capabilities. Significant superplasticity was observed at 516°C (960°F) where total elongation for strain rate of 2×10^{-4} S^{-} was as high as 650%. Measurements of the strain rate sensitivity, m, revealed corresponding maximum values in the range of 0.7 to 0.9. Measurements of m during constant strain rate tests indicate that m is only slightly sensitive to strain for true strain of at least 1.0.

Superplastic forming tests were also conducted utilizing commonly used gas pressure forming methods. Small demonstration parts were formed over a range of strain rates and thinning characteristics evaluated.

Metallographic evaluation of tensile test specimens and formed parts revealed the tendency of the alloy to form internal voids, or cavities, at large strains. The cavitation appears to be sensitive to the conditions of deformation, being minimized at the higher temperature and lower strain rates.

TABLES

TABLE OF CONTENTS

FOREWORD

This final technical report covers research conducted over the period from 1 October 1978 to 31 March 1979.

This contract with the Rockwell International Science Center, Thousand Oaks, California, was sponsored by the Department of the Army, ARRADCOM, Dover, New Jersey. It was administrated under the technical direction of Dr. J. Waldman, FC & SCUSL.

The program was managed for Rockwell International by Dr. C. H. Hamilton. The aluminum alloy sheet material was specially processed by the AlCOA Technical Laboratory, Pittsburgh, Pa. Technical assistance was provided by Mr. J. M. Curnow who conducted the forming experiments, Mr. L. F. Nevarez, who conducted the high temperature tensile testing. and Mr. M. Calabrese who conducted the metallographic effort.

FIGURES

FIGURES (Continued)

FIGURES (Continued)

INTRODUCTION

The ongoing need to cut cost and improve performance of ground and air vehicles continues to underscore the corresponding need for innovative developments in materials, processes, and design approaches. The added factor of increasing energy constraints suggests that such developments should include concentrated efforts in such lightweight materials as aluminum alloys. Superplastic forming of high strength aluminum alloys is believed to offer a significant potential advancement as a response to these needs if it can be realized.

Past experience in the superplastic forming of titanium alloys has demonstrated that enormous gains are possible by superplastic forming, provided that design concept is founded on the unique capabilities of the process (refs. 1-5). The major advantages observed in the superplastic forming of titanium alloys have been in the reduction of the number of parts and fasteners, and the corresponding reduction in the assembly costs. These observed advantages have resulted in an exponential increase in activity in this technology area over the past 5 years.

While the advantages are believed to be available to aluminum technology as well, one major factor has deterred its implementation. That factor is that high strength aluminum alloys are not superplastic in commercially produced forms whereas titanium alloys (especially the Ti-6Al-4V alloy) are quite superplastic in commercially produced sheet form. The reason for the lack of superplasticity in these aluminum alloys is the large grain sizes resulting from conventional processing. Typically, grain sizes are in excess of 20 μm and as high as several hundred microns, with most sheet products in a range of 30 to 100 μm.

Recent developments in thermomechanical processing methods have demonstrated that improved grain size control can be achieved. Early work by Di Russo et al. (refs. 6-7) resulted in the description of a technique, called an Intermediate Thermomechanical Treatment (ITMT), which was applied to Al-Zn-Mg-Cu (7075 Al) alloy. Subsequent developments by Waldman et al.

(refs. 8-11) resulted in the demonstration that 7000 series alloys can be recrystallized into a refined grain size by controlling the distribution of Cr as well as the major alloying elements Zn, Mg, and Cu. These processes focussed on plate forms and involved a relatively slow cooling sequence during the high temperature treatments.

Another technique was subsequently developed by Paton et al. (refs. 12,13) which involved the development of controlled size and spacing of soluble precipitates which then acted to nucleate recrystallization and concurrently restrict grain boundary migration during this recrystallization process. This technique, which has been demonstrated on a wide range of precipitation hardening alloys, has permitted the development of stable grain sizes of about 10 μm in a number of aluminum alloys.

With such a fine grain structure, high temperature deformation characteristics approaching superplastic behavior have been indicated for several 7000 series aluminum alloys. This program was, therefore, conducted to assess the potential for achieving superplasticity and superplastic forming characteristics of a selected aluminum alloy, 7475, processed by the thermomechanical treatment (refs. 12,13) to develop a fine grain structure.

This program, therefore, involved the evaluation of elevated temperature deformation characteristics, grain size and grain size stability, and a preliminary evaluation of the superplastic formability of the material.

PROGRAM OBJECTIVES

The objectives of this program are to assess the superplastic properties and superplastic forming capability of a fine grained 7475 Al alloy over a range of strain-rates and temperatures.

EXPERIMENTAL

In this program 7475 aluminum (Al) alloy sheet was produced by a commercial supplier utilizing processing conditions in accordance with prescribed

requirements in an effort to produce a very fine grain size. This fine grained aluminum alloy sheet was then evaluated for its grain size and grain size stability at high temperatures, and its superplastic properties were evaluated by conducting tensile tests at elevated temperatures. Based on these data, preliminary superplastic forming tests were conducted in which samples of the fine grained aluminum sheet were formed using gas pressure at elevated temperatures. The forming parameters evaluated were then based upon the properties of the material determined in the previous tensile tests. This program was, therefore, designed to provide a preliminary evaluation of the potential for superplastic forming this fine grained 7475 Al alloy.

Material

The 7475 Al alloy evaluated in this program was specially processed by the ALCOA Technical Laboratory utilizing the thermomechanical processing parameters prescribed to achieve a fine grain size. The starting material to be specially processed was 2.54 cm (1 in.) thick plate material which had been conventionally processed to plate thickness. This material was then thermomechanically processed down to the final gage of approximately 0.254 cm (0.1 in.). The special processing conditions used for the sheet were to first of all solution treat the material, after which it was given an over-aged treatment at 400°C (752°F) for 8 hours, followed by rapid cooling to room temperature. The material was then warm rolled at 204°C (400°F) to a final sheet thickness dimension of 0.254 cm (0.1 in). Temperatures during the rolling procedure were allowed to decrease until the final rolling passes on the sheet were conducted at ambient temperature. This sheet material was supplied to Rockwell International Science Center in the as-rolled condition. Prior to further testing and forming evaluations, this material was then recrystallized at 482°C (900°F) for 15 minutes in a salt bath.

This thermomechanical procedure has been shown to be quite effective in refining the grain size of precipitation hardenable aluminum alloys. That is, micromechanisms active in achieving the grain refinement involve the control of the size and spacing of the soluble precipitate, which acts to nucleate recrystallization as well as to impede grain boundary migration during the

recrystallization process. The precipitate particles formed during the over-aging treatment are of the order of a micron in diameter and several microns separated. During the warm working (i.e., rolling at or below 204°C (400°F)), dislocation structures develop with an increased concentration at the particles. On exposure to the recrystallization temperature, this concentrated dislocation structure immediately adjacent to the particles form nucleation sites for the recrystallization process. Because of their relatively close spacing, a high density of nuclei form, leading to a correspondingly small grain size. The presence of precipitate particles also acts to impede grain boundary migration during recrystallization, further aiding in maintaining a fine grain size.

Grain Growth Kinetics

The grain size resulting from this process for the 7475 Al alloy measured approximately 7.8 μm in a short transverse dimension and approximately 14 μm in the rolling direction and the long transverse direction. The stability of this fine grain structure at elevated temperatures was also evaluated by exposing metallographic sections of samples to various elevated temperatures for times from 15 min to as long as 24 hr. Exposure temperatures included 427°C (800°F), 454°C (850°F), 482°C (900°F), 493°C (920°F), and 516°C (960°F). The length of exposure times at these temperatures included 15 min, 1 hr, 4 hr, 8 hr, and 24 hr. Samples were heat treated in a salt bath and, following exposure to various temperature-time combinations, were water quenched and then examined metallographically. Since the dimensions of the grains in the long transverse and longitudinal directions were found to be identical, the grain measurements for these grain growth tests were taken only for the short transverse dimension and the longitudinal dimension. Results of this grain growth kinetics study are summarized in table 2 and in fig. 1. It is apparent from these data that the fine grain size developed by this special processing is quite stable even at temperatures as high as 516°C (960°F) over the longest times evaluated, that time being 24 hr. An example of the microstructures resulting from the high temperature grain growth studies are shown in fig. 2 for the times of 15 min, 1 hr, 4 hr, 8 hr, and 24 hr.

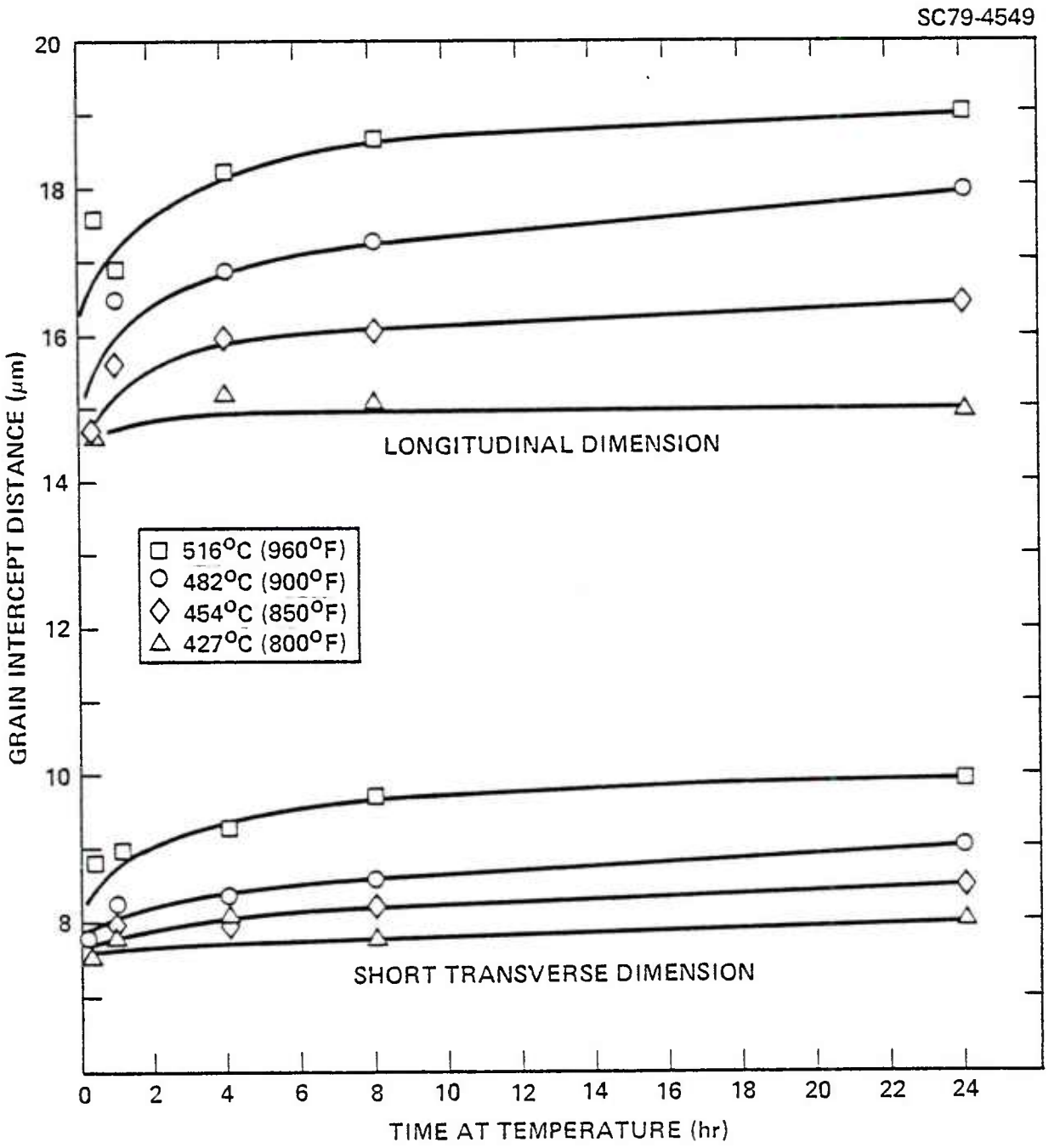

Figure 1. Grain intercept distance as a function of exposure time at elevated temperature for 7475 aluminum alloy.

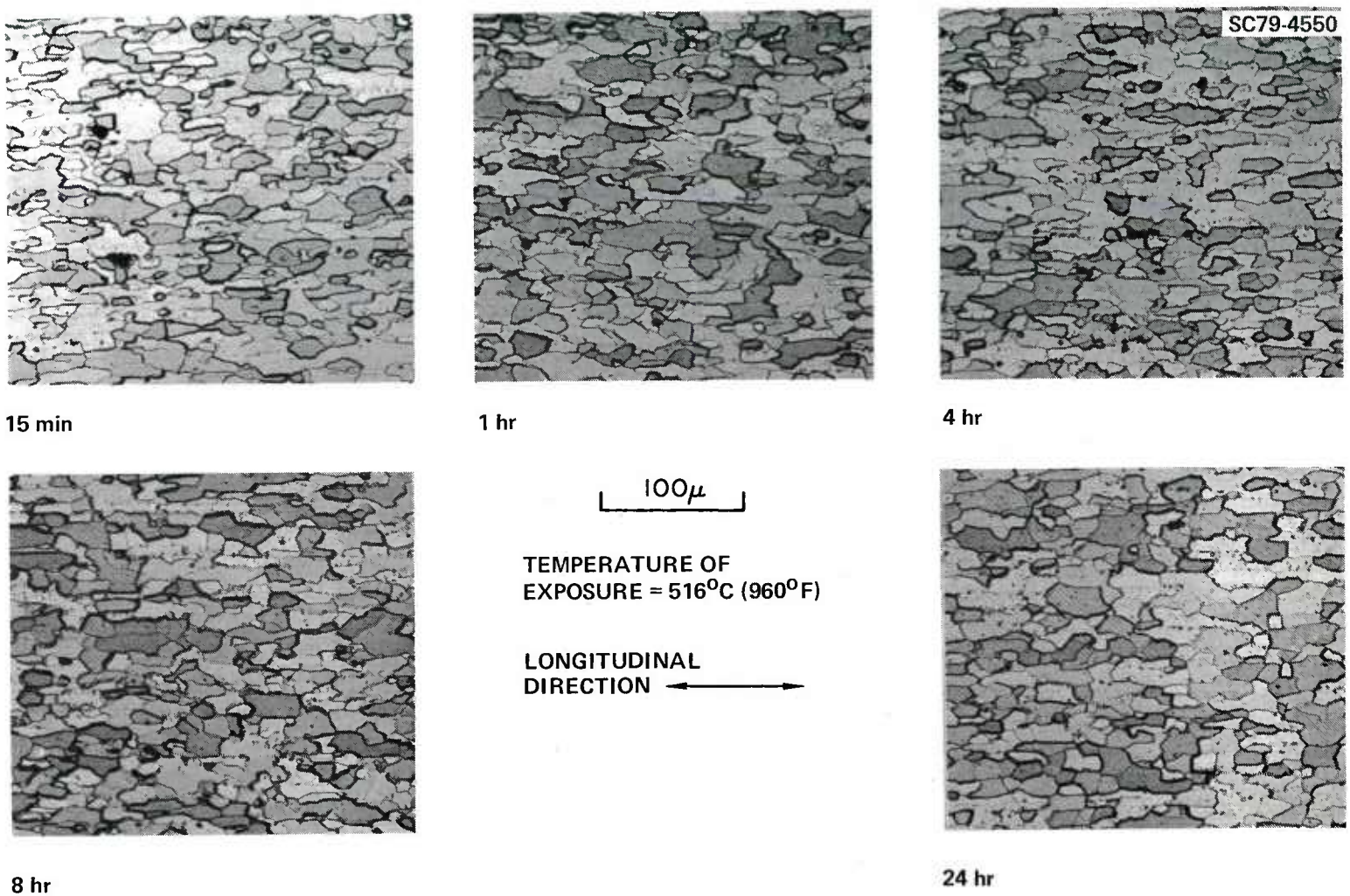

Figure 2. Optical micrographs of 7075 aluminum alloy after exposure to 516°C (960°F) for times of from 15 mins to 24 hours.

The grain size measurements made for this material were performed on optical micrographs taken at 250X magnification. The measurements were determined using a linear intercept method and a minimum of 100 intercepts were counted for each orientation of each microstructure.

High Temperature Tensile Tests

The superplastic properties of this fine grained aluminum alloy were evaluated at elevated temperatures by tensile testing to determine the strain-rate sensitivity of the flow stress for the material, and also to determine the stress-strain characteristics for the material and tendencies to strain harden. Tensile tests were conducted in air using a test specimen consisting of an overall dimension measuring 10.16 cm (4 in.) in overall length with a gage section of 2.54 cm (1 in.) in length and a width of the test section being 0.953 cm (0.375 in.).

Step strain-rate tests were used to determine the strain-rate sensitivity of flow stress in which a single tensile specimen was utilized and the cross-head speed incrementally increased during the testing to impose varying strain-rates. This technique has been discussed in detail elsewhere (refs. 14 and 15). These tests were conducted at temperatures of 371°C (700°F) , 427°C (800°F), 482°C (900°F), and 516°C (960°F); both longitudinal and long transverse test directions were evaluated using this technique. A five zone split furnace was used to heat the tensile specimens, and the temperature gradient within the test area was held to within ±2°C.

Results of these step strain-rate tests are shown in figs. 3 and 4 where log flow stress is presented as a function of the log strain-rate. The strain-rate sensitivity exponent, m, for these data was determined from the curves of figs. 3 and 4 by means of measuring the slopes of the curves fitted through the data. The resulting curves of the m values for these data are presented as a function of the log strain-rate for the various temperatures during testing in figs. 5 and 6.

From these data, it is apparent that the strain-rate sensitivity of the flow stress for the fine grain 7475 Al alloy is highest at a temperature of

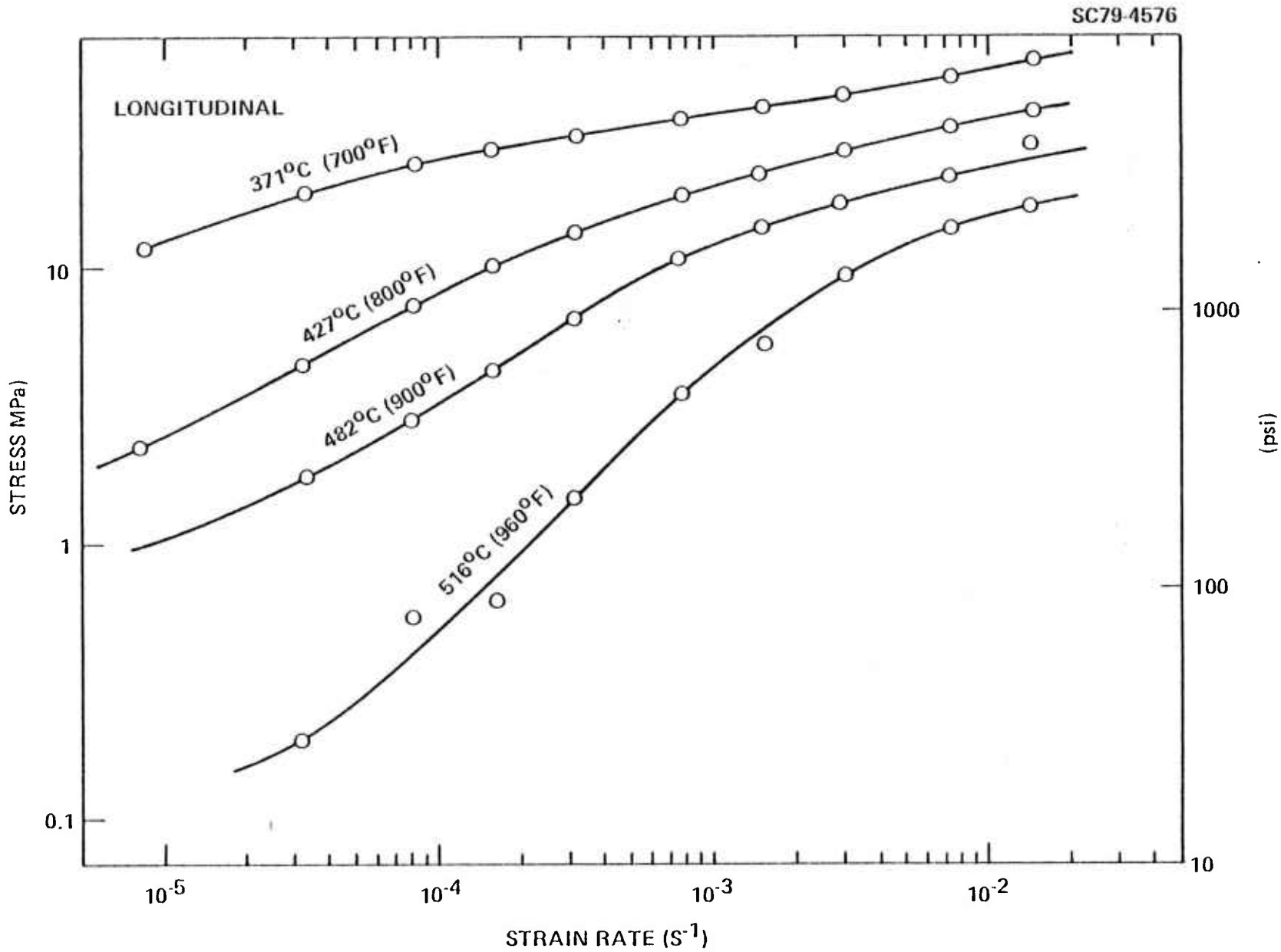

Figure 3. Flow stress as a function of applied strain-rate for the /4/5 aluminum alloy tested in the longitudinal direction at four elevated temperatures.

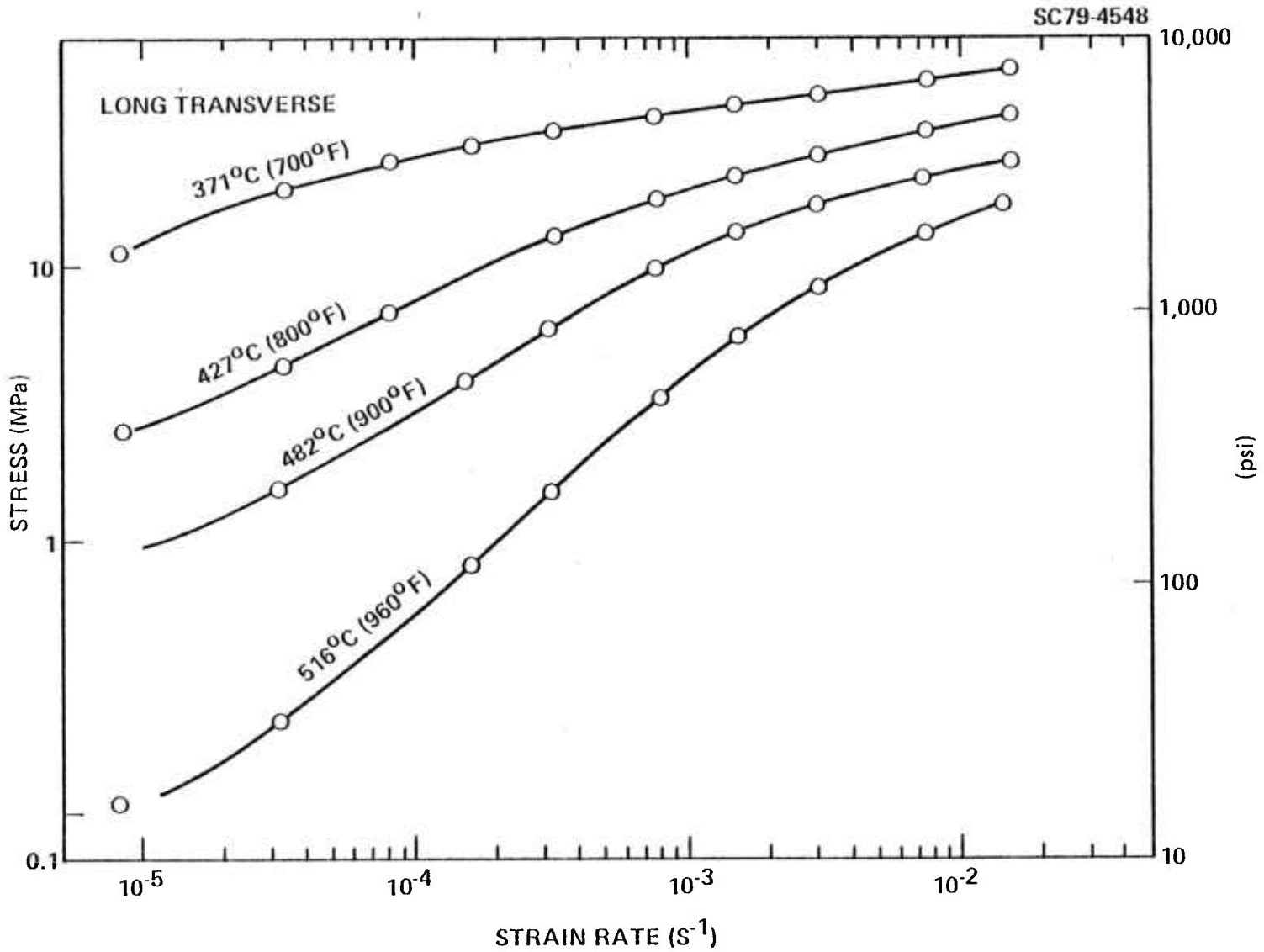

Figure 4. Flow stress as a function of applied strain-rate data for the 7475 aluminum alloy tested in the long transverse direction at four elevated temperatures.

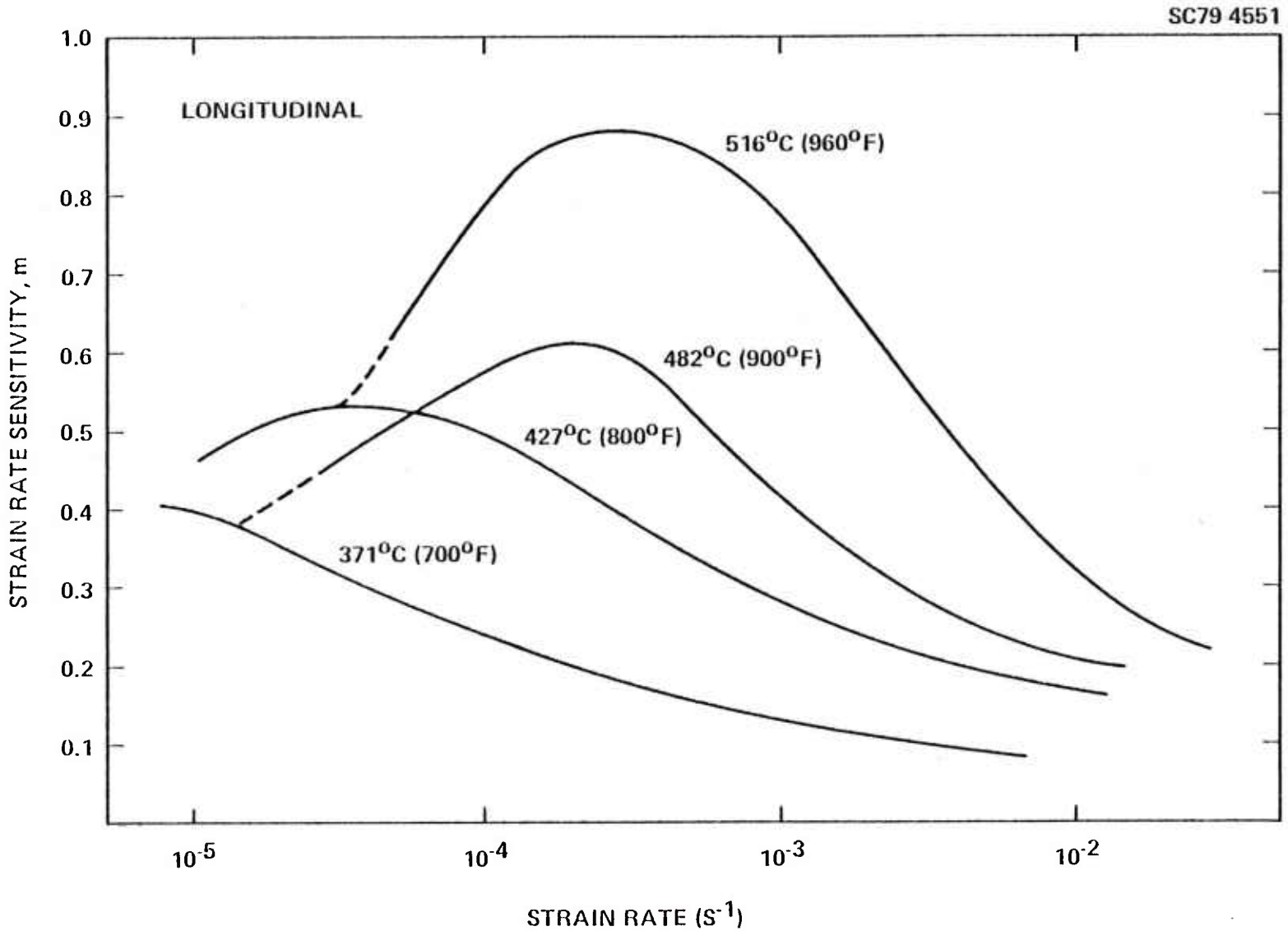

Figure 5. Strain rate sensitivity, m, as a function of strain-rate for the 7475 aluminum alloy tested in the longitudinal direction. Values determined from the data shown in fig. 3.

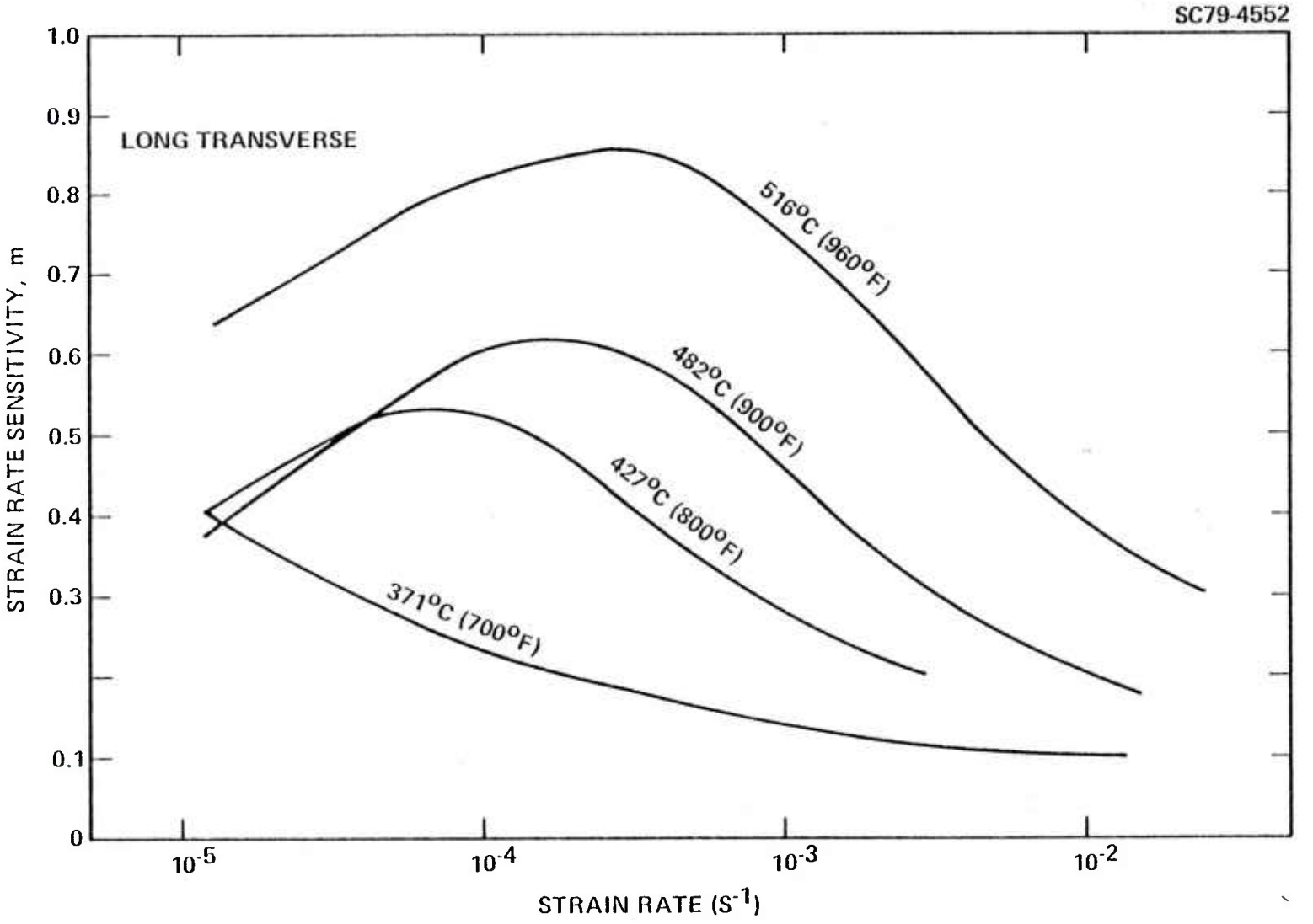

Figure 6. Strain rate sensitivity, m, as a function of strain-rate for the 7475 aluminum alloy tested in the transverse direction. Values determined from the data in fig. 4.

516°C (960°F) and reaches a peak at the strain-rate of about 4×10^{-4} s^{-1}. The flow stress properties and the m values for the material appear to be independent of the test direction indicating that the material, in terms of the superplastic properties, at least, is isotropic.

In order to further evaluate the high temperature deformation characteristics and superplastic forming potential for the material, additional testing was conducted in which constant strain-rate was imposed on the samples. Samples were strained to failure under constant strain-rate in order to measure the total elongation capability of the materials at a given strain-rate and temperature. During these tests, flow stress data were taken so that the stress-strain characteristics could be established in order to determine the extent of hardening, if any, that occurs during the straining of the material. Tests were performed at the two temperatures of 482°C (900°F) and 516°C (960°F). Since the step strain-rate data suggested that these two temperatures should offer the greatest potential for superplastic deformations, the strain-rates imposed on the samples varied from 10^{-2} s^{-1} to 2×10^{-4} s^{-1} for both test temperatures. The equipment and procedures used to conduct the constant strain-rate tests were described in ref. 13. Both longitudinal and long transverse tests were conducted for the material.

The results of these constant strain-rates are presented in fig. 7 for the 482°C (900°F) test temperature and in fig. 8 for 516°C (960°F) for the longitudinal test specimens. In these figures the true stress is plotted as the function of true strain up to the true strain level of 1.0 corresponding to about 178% tensile elongation. Although the extent of the strain hardening of the materials is not great, it appears, that hardening does occur. The extent of hardening at 482°C (900°F), particularly at the lower strain-rate, is noticeably greater than for 516°C (960°F). At strain-rates of 5×10^{-3} s^{-1} and 10^{-2} s^{-1} at both temperatures rapid fluctuations in load were observed during straining, and are represented in these curves by the cross-hatched band in the stress strain curves. It is likely that dynamic strain aging is occurring during the the higher strain-rates causing rapid variation in the flow stress. The maximum flow stress followed by a drop in the curve for several of the higher strain-rates is believed to be due to the development of

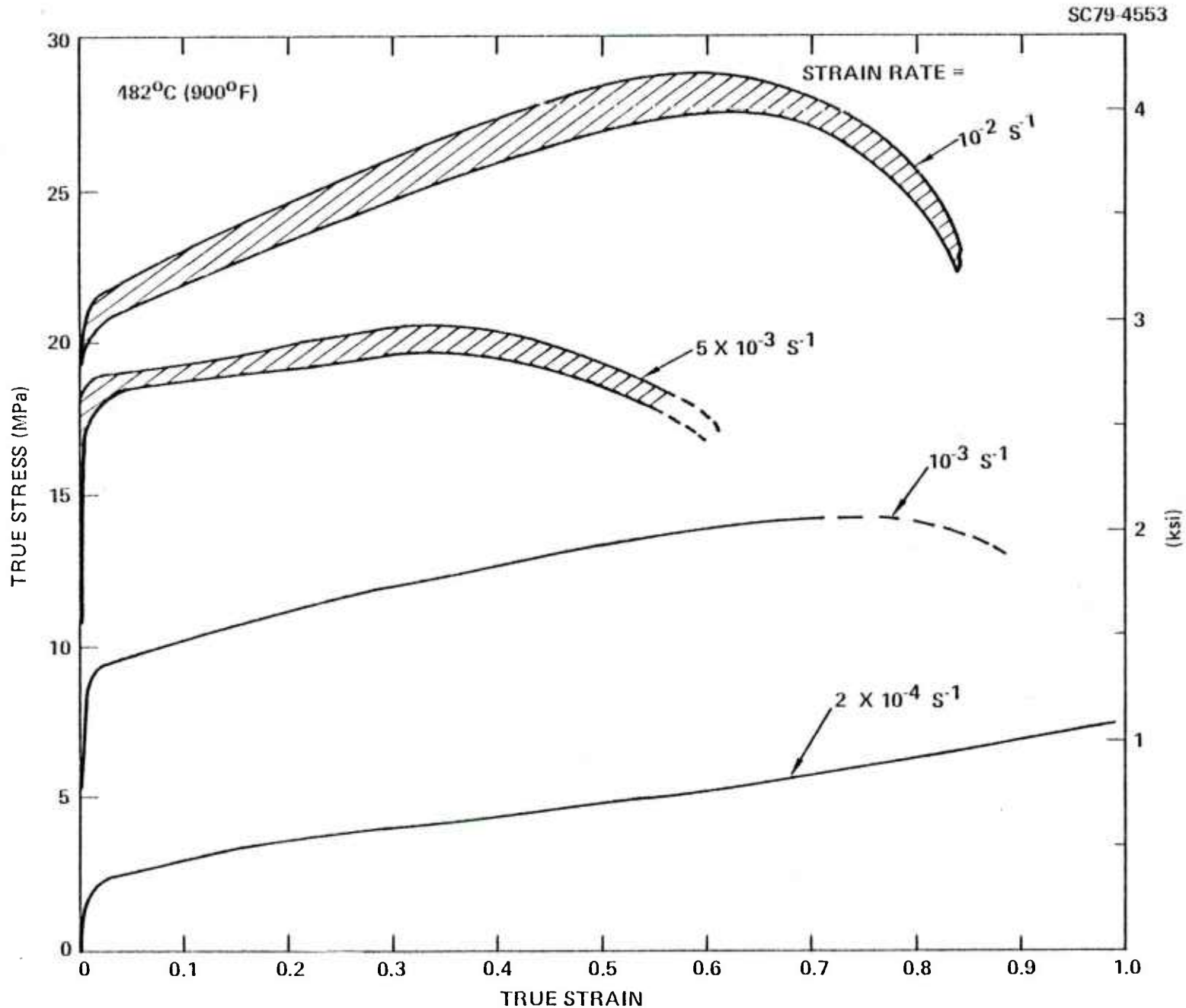

Figure 7. True stress as a function of true strain for constant strain-rate tests at the temperature of 482°C (900°F).

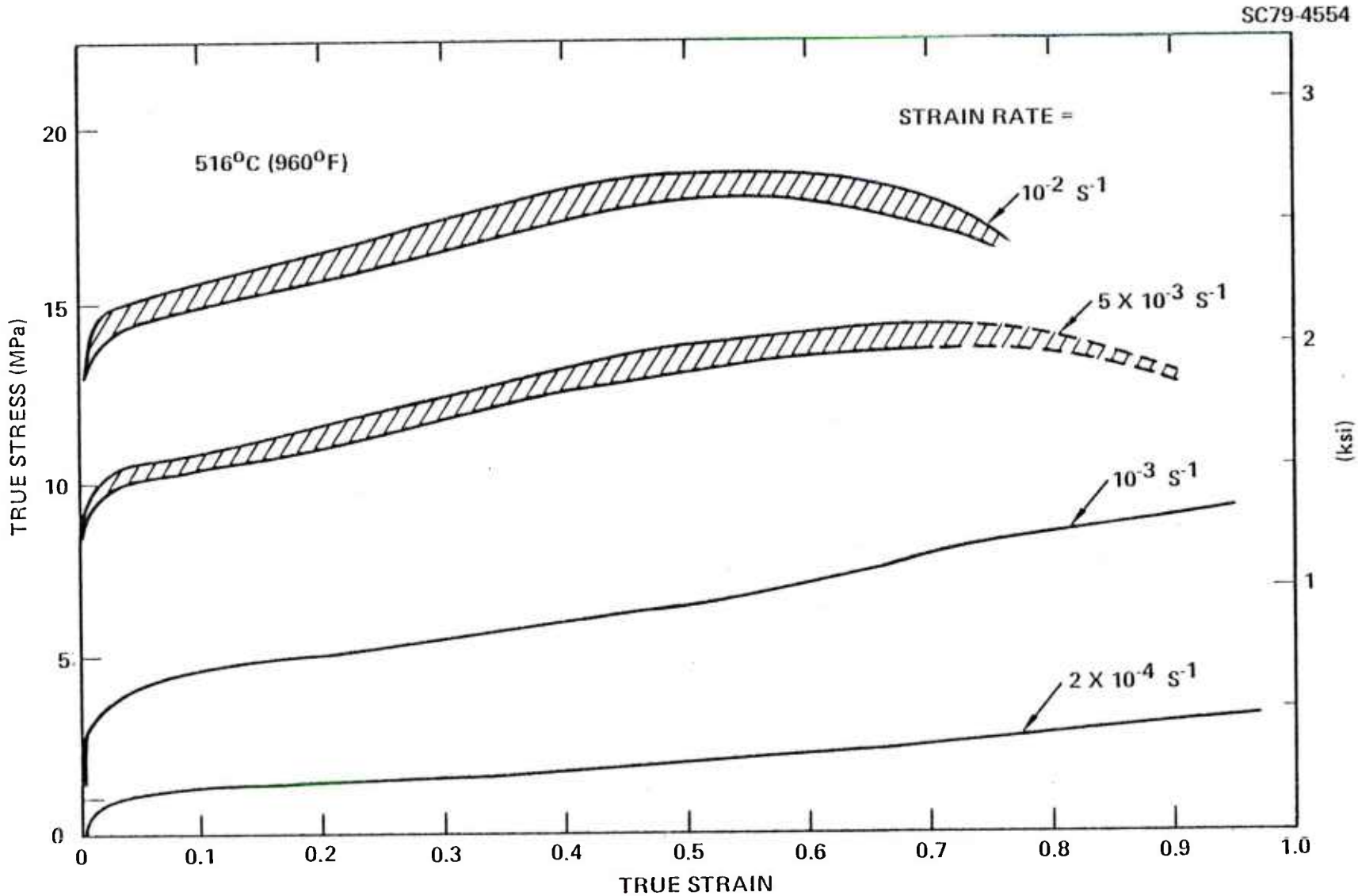

Figure 8. True stress as a function of true strain for constant strain-rate tests conducted at 482°C (900°F).

local instabilities in the test section leading to imminent fracture. This development of an instability can then cause an apparent loss, or drop, in true stress which is not actually indicative of the stress-strain characteristics of the material at these strains.

The total elongations measured for these test specimens are presented in table 3. The largest elongation observed was 650% measured at 516°C (960°F) for a strain-rate of 2×10^{-4} s^{-1}. Significant elongations were observed at strain-rates as high as 10^{-3} s^{-1} for this temperature in which values of 275% to more than 450% elongation were measured. These ductilities are significantly higher than those observed for the temperature of 482°C (900°F) where the maximum tensile elongations measured were on the order of 300% for the strain-rate of 2×10^{-4} s^{-1}. An example of a test specimen is shown in fig. 9. In this figure a test specimen strained to more than 500% tensile elongation at a temperature of 516°C (960°F) and a strain-rate of 2×10^{-4} s^{-1} is shown in comparison with the as-machined test specimen. The samples were marked by electro-etching techniques with circles of the diameter of 0.254 cm (0.1 in.) to provide a measure of the local strain distribution along the test specimen.

Step strain-rate tests provide a measure of the strain-rate sensitivity of flow stress of the material at relatively low total strains. However, those tests do not necessarily provide a valid measure of m for large strains and, therefore, cannot provide a complete picture of the flow characteristics, particularly if m decreases with deformation. A test method that better evaluates the variability of the strain-rate sensitivity, m, is that test described in ref. 15, which involves constant strain-rate testing during which small local changes in the strain-rate are imposed to provide for a measure of the strain-rate sensitivity m. This technique permits a local step in strain-rate at a number of different strains for which the strain-rate sensitivity can then be computed. This technique is illustrated in fig. 10 where the load as a function of deformation is shown. For these tests the strain-rate was increased temporarily by 40% and sustained at that increased strain-rate for a period sufficient to develop a clear definition of the flow stress for the higher strain-rate, after which the original strain-rate was subsequently

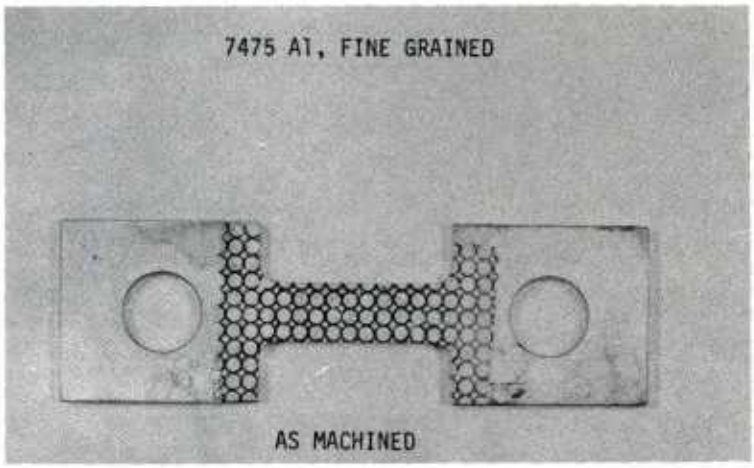

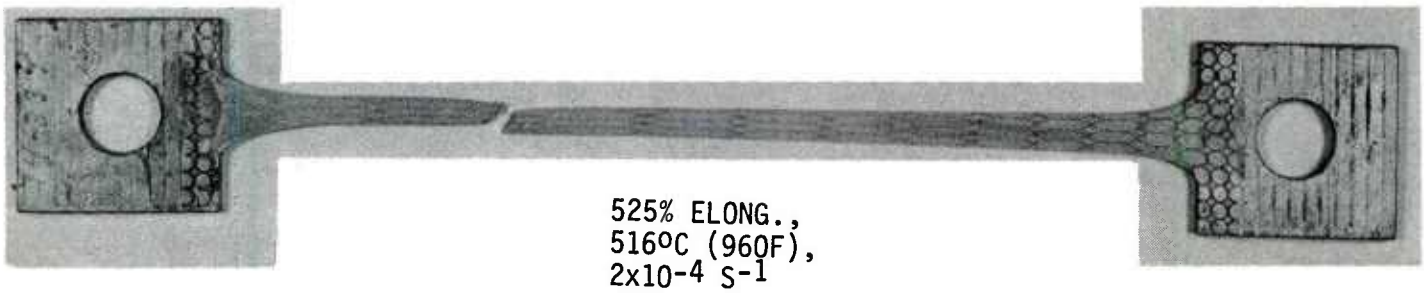

Figure 9. Tensile test specimen before and after total elongation tests at 516°C (960°F) under a constant strain-rate of 2×10^{-4} s^{-1} power.

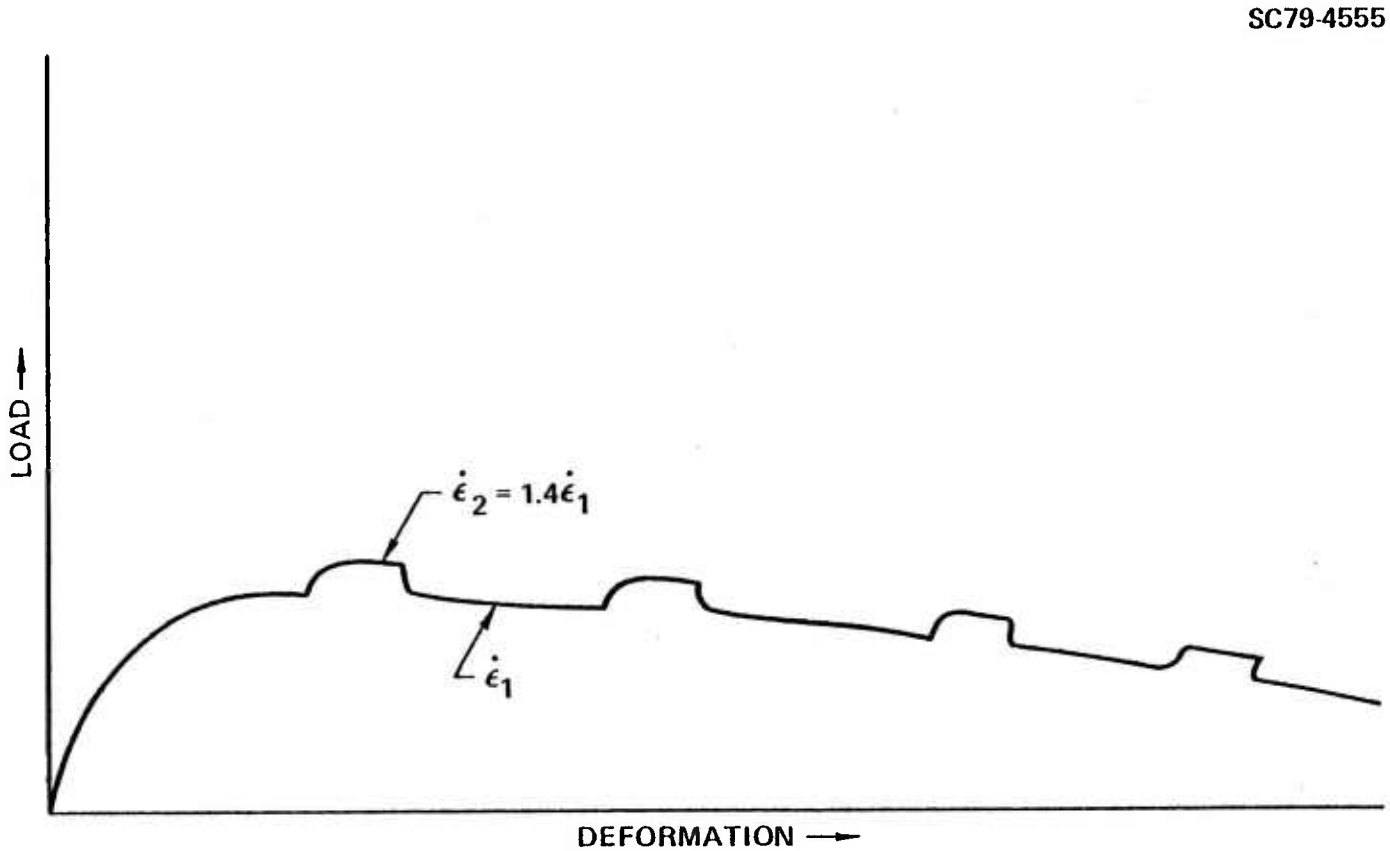

Figure 10. Schematic illustration of the load vs. deformation under constant strain-rate testing showing the effect of local increases in strain-rate to facilitate determination of m as a function of strain.

imposed and continued until the next step in strain-rate was conducted. This technique was utilized for strain-rates of 2×10^{-4} s^{-1} and 10^{-3} s^{-1} for both temperatures. However, because of the appearance of dynamic strain aging, and problems associated with changing strain-rates at the higher strain-rates of 5×10^{-3} and 10^{2} s^{-1}, it was not possible to make these measurements at those strain-rates.

The resulting strain-rate sensitivity measurements are shown in fig. 11 for a strain-rate of 2×10^{-4} s^{-1} and in fig. 12 for 10^{-3} s^{-1}. At the temperature of 516C (960°F) the m value appears to be quite constant at about 0.75 for the true strain of up to 1.0. At a temperature of 482°C (900°F), the m value appears to decay somewhat more rapidly than for the higher temperature; however at both temperatures there appears to be very little loss in the m value for a strain of at least 1.0. For a strain-rate of 10^{-3} s^{-1}, it appears that there is a somewhat more rapid decay in the m value for both temperatures although at the temperature of 482°C (900°F) there appears to be more rapid decrease in the strain-rate sensitivity exponent m.

The test sections of the tensile specimens on which the total elongation tests were conducted were examined metallographically, and micrographs corresponding to these specimens are shown in figs. 13 and 14 for tests conducted at 516°C (960°F) and figs. 15 and 16 for 482°C (900°F). The strain-rates and the strain level at which the metallographic section was taken are indicated below each of the optical micrographs. The grain sizes were measured on the samples after testing and are presented in table 4. Also presented in table 4 are the corresponding grain sizes which would be expected based on the grain coarsening study shown in fig. 1. One feature which was observed in these tensile specimens is evidence of cavitation or internal void formation. Examples of the cavitation can be seen in figs. 13 and 14.

The grain size characteristics summarized in table IV indicate that the grain size stability of these materials remains good even during the conditions of deformation. There is some evidence of dynamic recrystallization occurring with some grain refinement resulting at the strain-rate of 5×10^{-3} s^{-1} and at 516°C (960°F). For this test condition the dimensions of

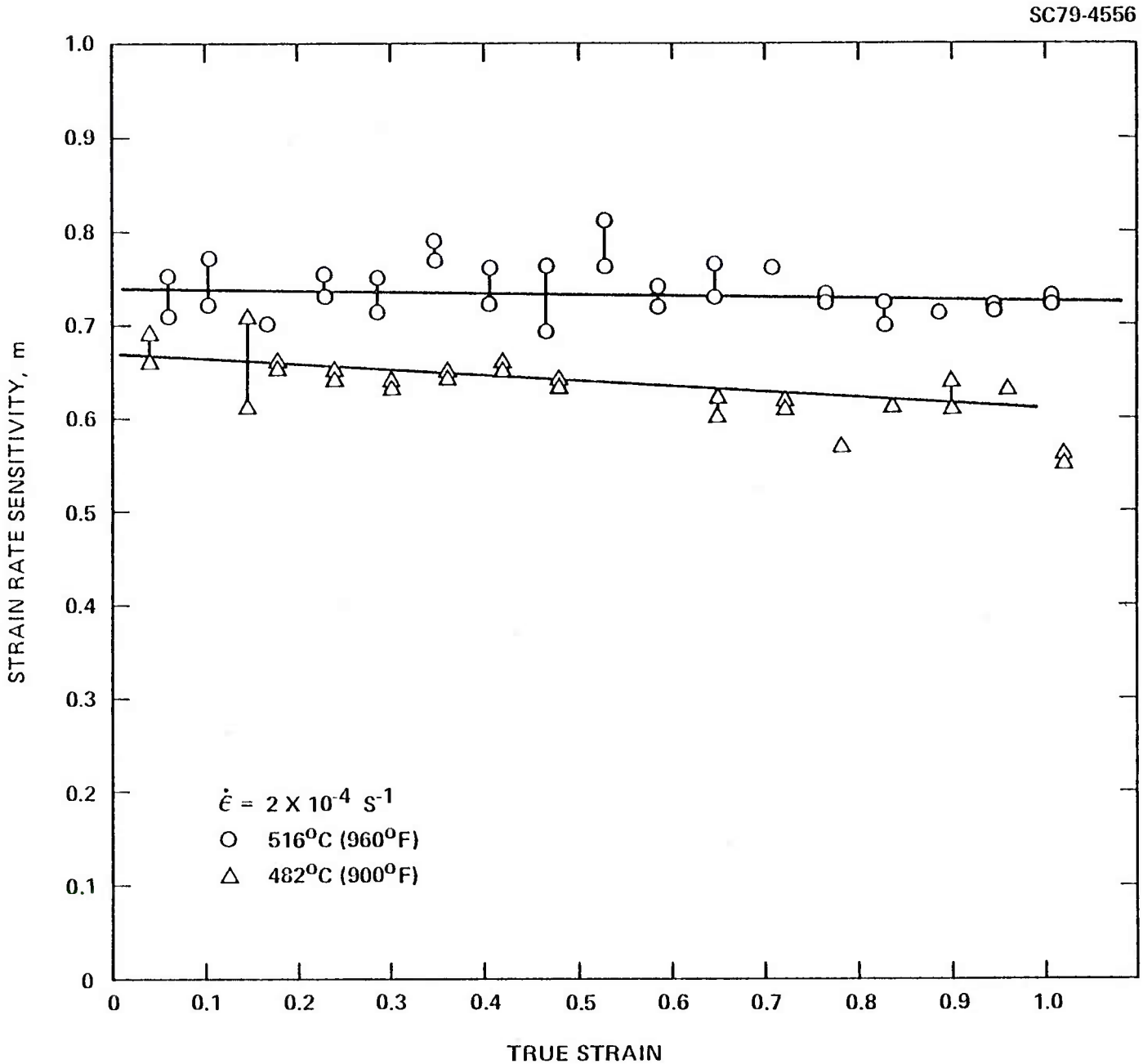

Figure 11. Strain rate sensitivity, m, as a function of true strain for a constant strain-rate of 2×10^{-4} s^{-1} at temperatures of 516°C (960°F) and 482°C (900°).

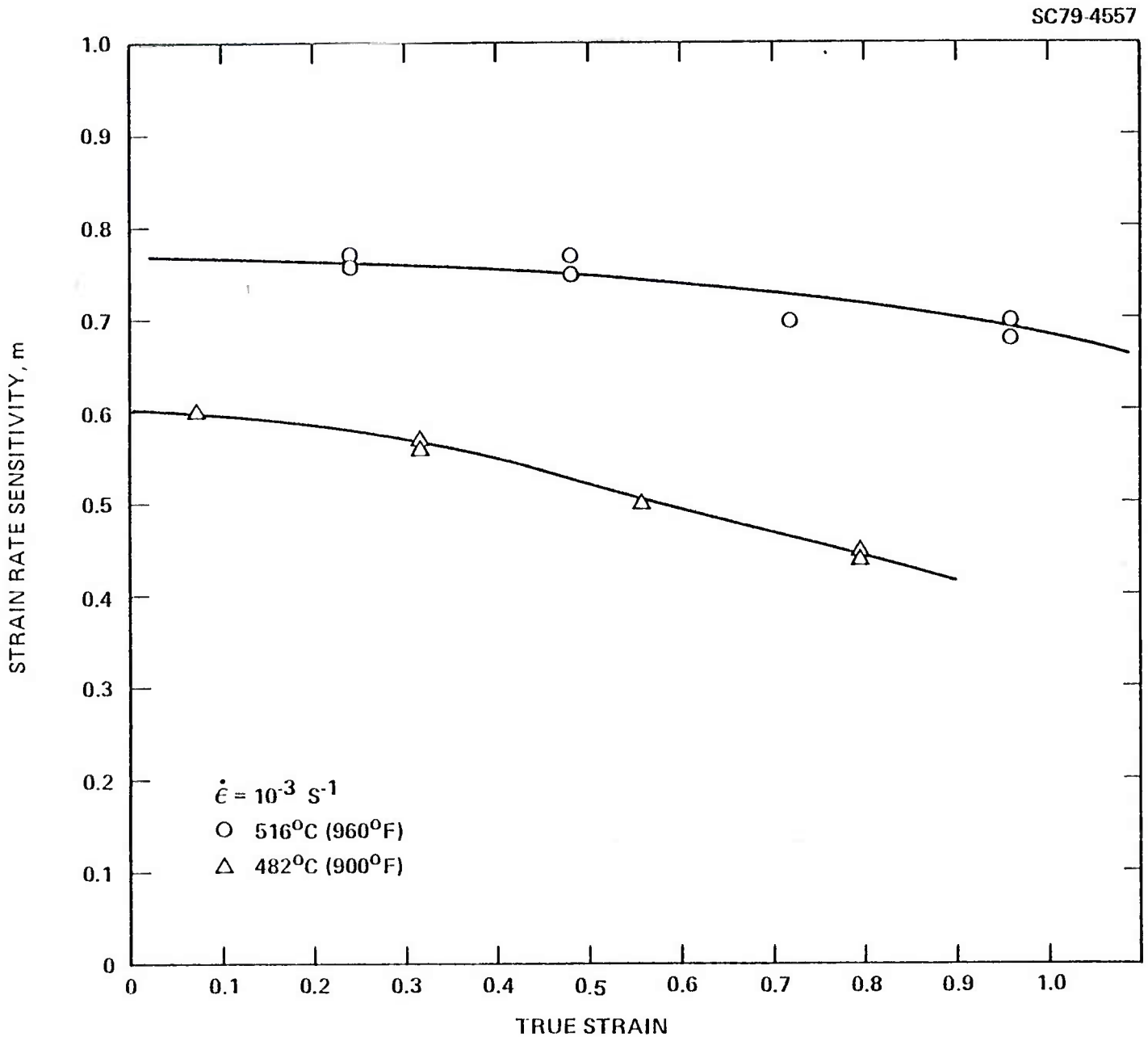

Figure 12. Strain rate sensitivity, m, as a function of true strain for a constant strain-rate of 10^{-3} s^{-1} of temperatures of 516°C (960°F) and 482°C (900°F).

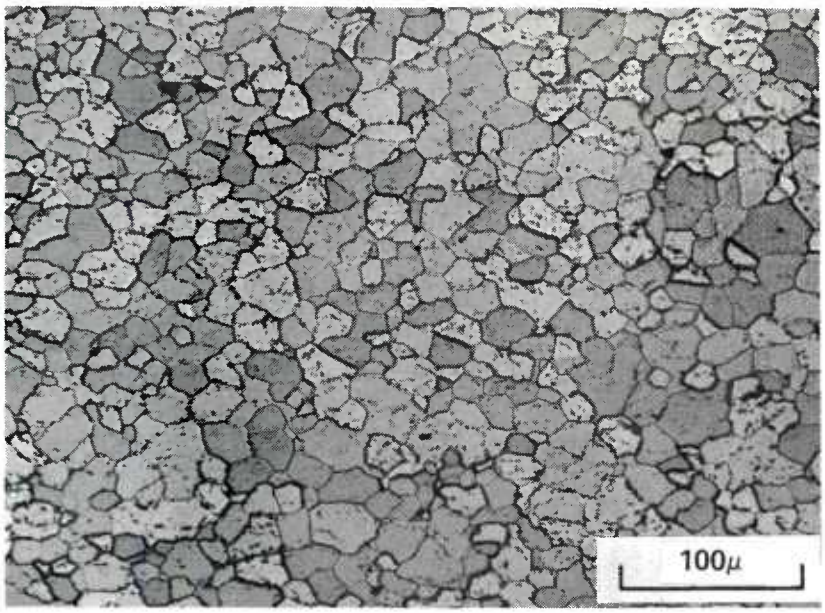

$\dot{\epsilon} = 5 \times 10^{-5}$
$\epsilon = 1.77$

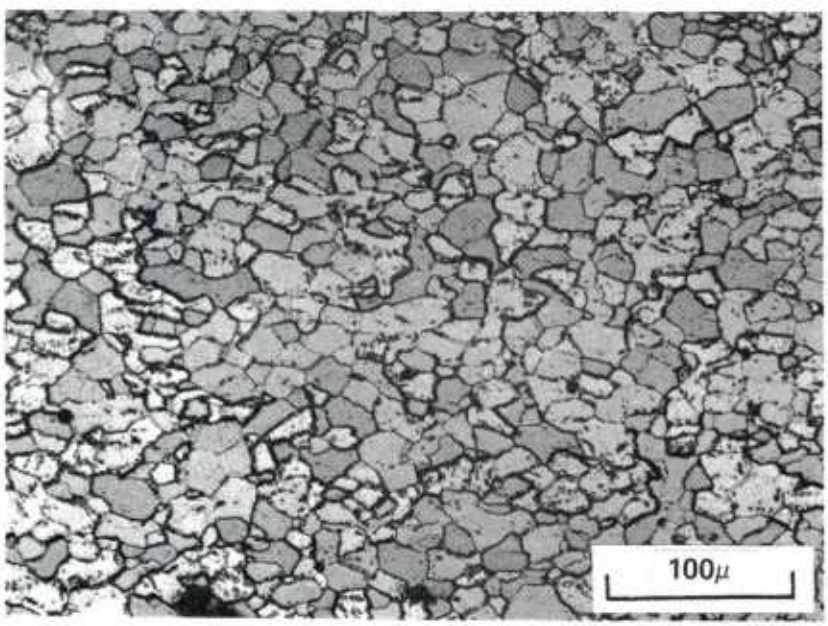

$\dot{\epsilon} = 2 \times 10^{-4}$
$\epsilon = 1.77$

Figure 13. Optical micrographs of 7475 aluminum alloy from total elongation specimens tested at 516°C (960°F).

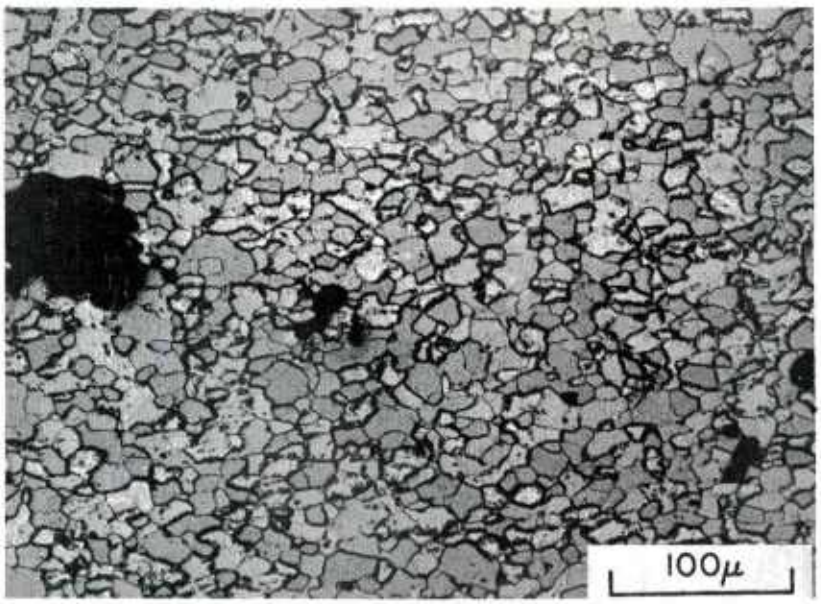

$\dot{\epsilon} = 10^{-3}\ s^{-1}$
$\epsilon = 1.39$

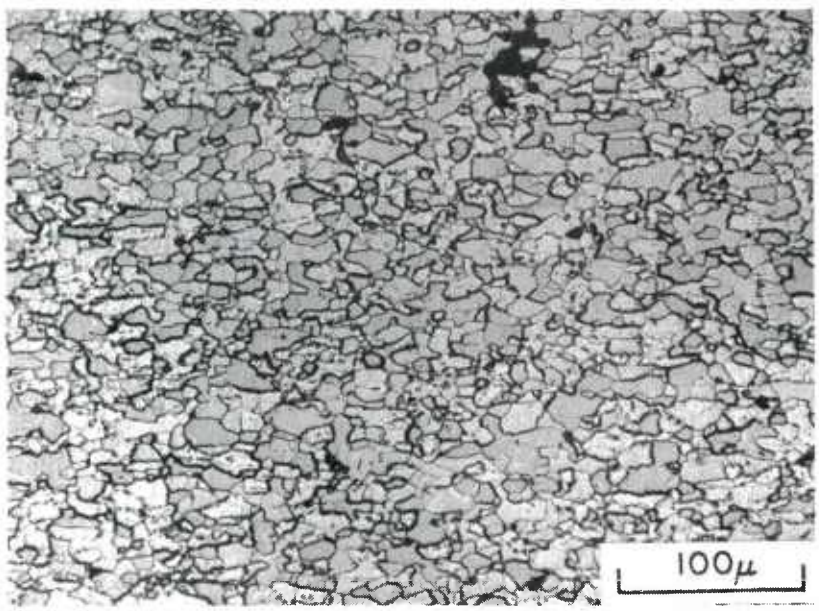

$\dot{\epsilon} = 5 \times 10^{-3}$
$\epsilon = 1.04$

Figure 14. Optical micrographs of 7475 aluminum alloy from total elongation specimens tested at 516°C (960°F).

SC79-4560

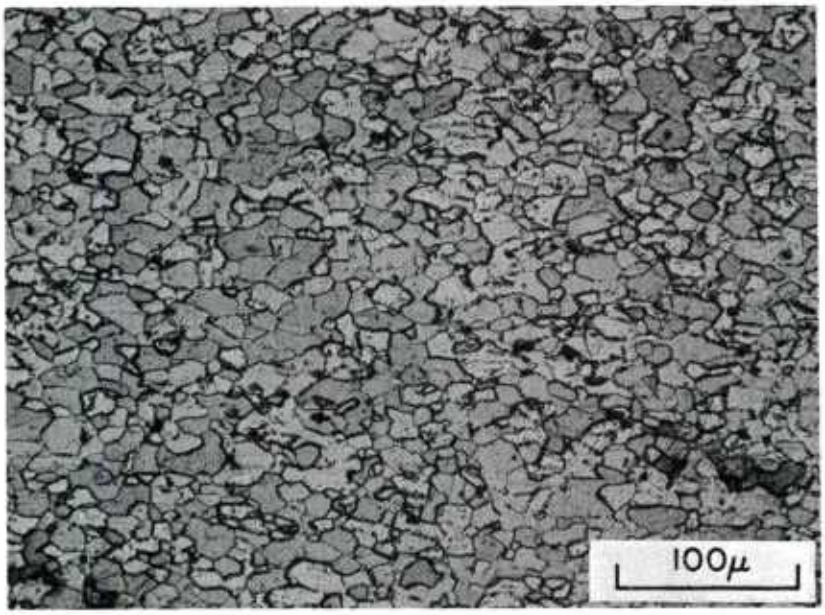

$\dot{\epsilon} = 2 \times 10^{-4}\ s^{-1}$
$\epsilon = 1.43$

Figure 15. Optical micrographs of 7475 aluminum alloy from total elongation specimens tested at 482°C (900°F).

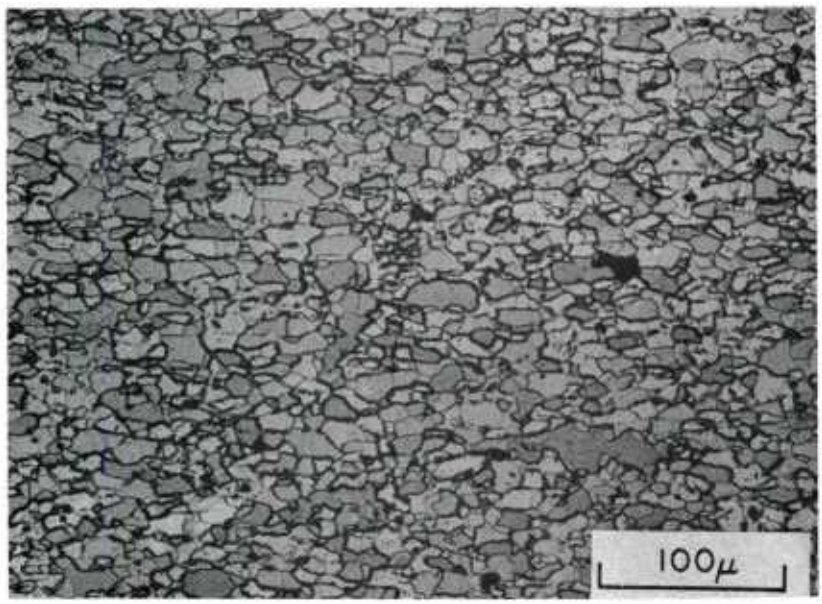

$\dot{\epsilon} = 10^{-3}\ s^{-1}$
$\epsilon = 1.09$

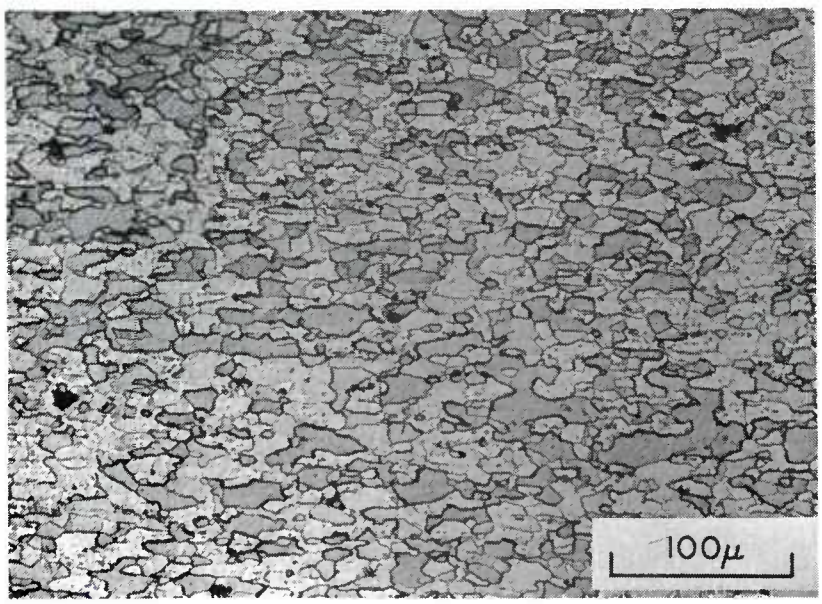

$\dot{\epsilon} = 5 \times 10^{-3}$
$\epsilon = 0.69$

Figure 16. Optical micrographs of 7475 aluminum alloy from total elongation specimens tested at 482°C (900°F).

the grains in both the short transverse and longitudinal direction were reduced noticeably. This reduction in grain size is also apparent in fig. 14 for that strain level.

Superplastic Forming Tests

From the basis of the high temperature tensile test results, superplastic forming evaluation tests were designed to further demonstrate that this material could be superplastically formed using the gas pressure superplastic forming method. Forming tests were conducted on the fine grain 7475 aluminum alloy sheet material at temperatures of 516°C (960°F) and 482°C (900°F). The test parts evaluated were of a rectangular pan configuration with overall dimensions of 10.16 cm (4 in.) by 20.32 cm (8 in.), and the formed section measured 5.08 cm across (2 in.) by 2.54 cm (1 in.) deep by 15.14 cm (6 in.) in length. Alternate forms were also produced in which the depth of the cavity was changed to 1.27 cm (1/2 in.) in depth, and a specially designed configuration to demonstrate the unique capability of the process in which a bead configuration was formed in the bottom of the rectangular part along with a large step or joggle on one end and an impression of a logo on the bottom of the part.

The gas pressure vs. time schedules used on the parts were developed with an intent to control the rate of deformation to an approximately constant strain-rate for the free forming sections of the part. This pressure-time schedule is illustrated in fig. 17 for the 2.54 cm (1 in.) deep test parts and in fig. 18 for the 1.27 cm (1/2 in.) deep test parts. Since variations in temperature and intended strain-rates cause corresponding variations in the applied pressures and times for forming, these parameters have been identified in fig. 17 as pressures p_1 and p_2, and the corresponding times t_{total} and t_{hold}, which are then summarized in table 5 for the range of parts fabricated. A change in depth of the part changes the pressure profiles substantially as shown in fig. 18 for the shallow parts.

The imposed pressure profiles generated a range of strain-rates as shown in table 5 for the various parts fabricated. Strain rates imposed ranged from

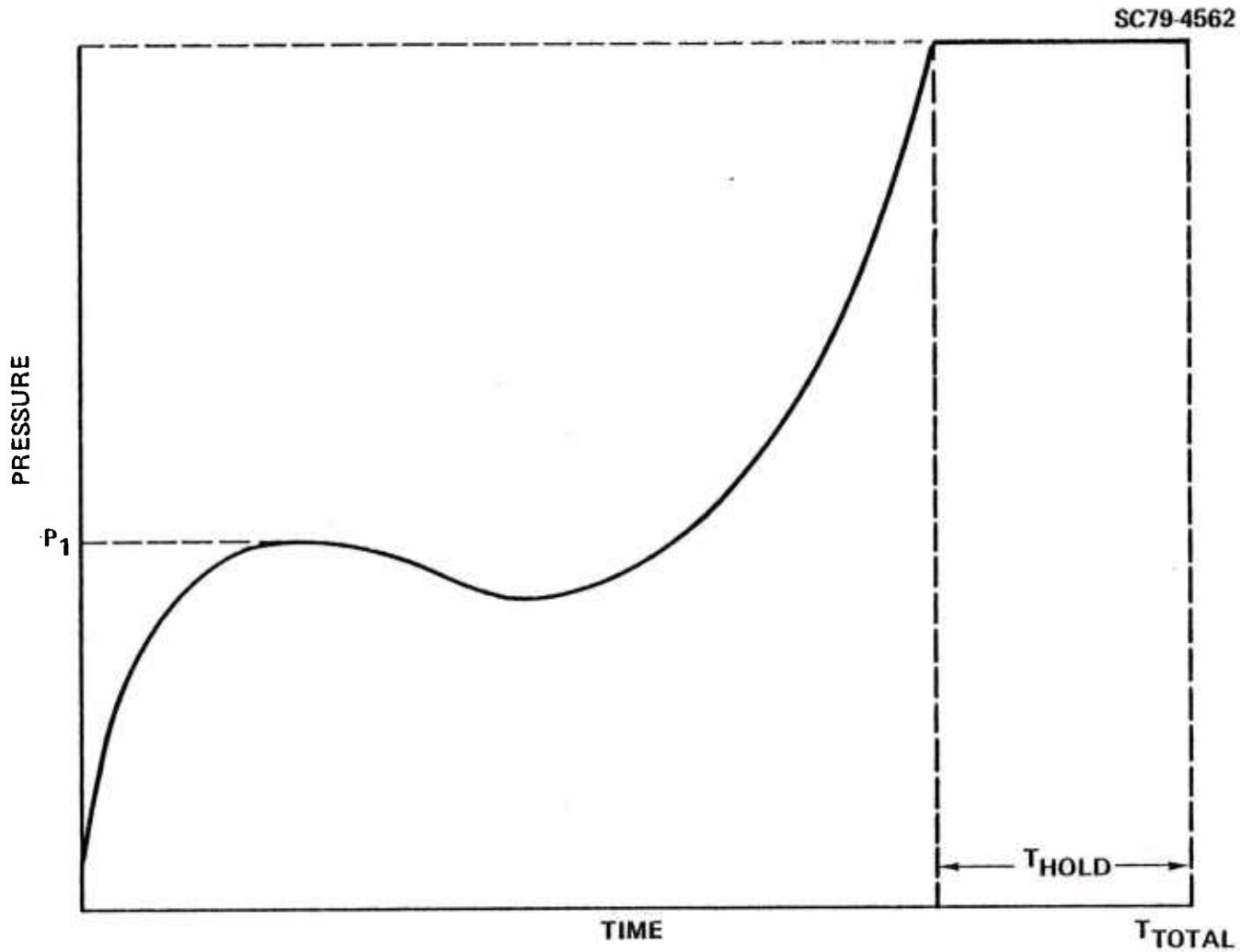

Figure 17. Pressure/time profile for 2.54 cm (1 in.) deep superplastically formed test parts. See table 5 for actual pressures used.

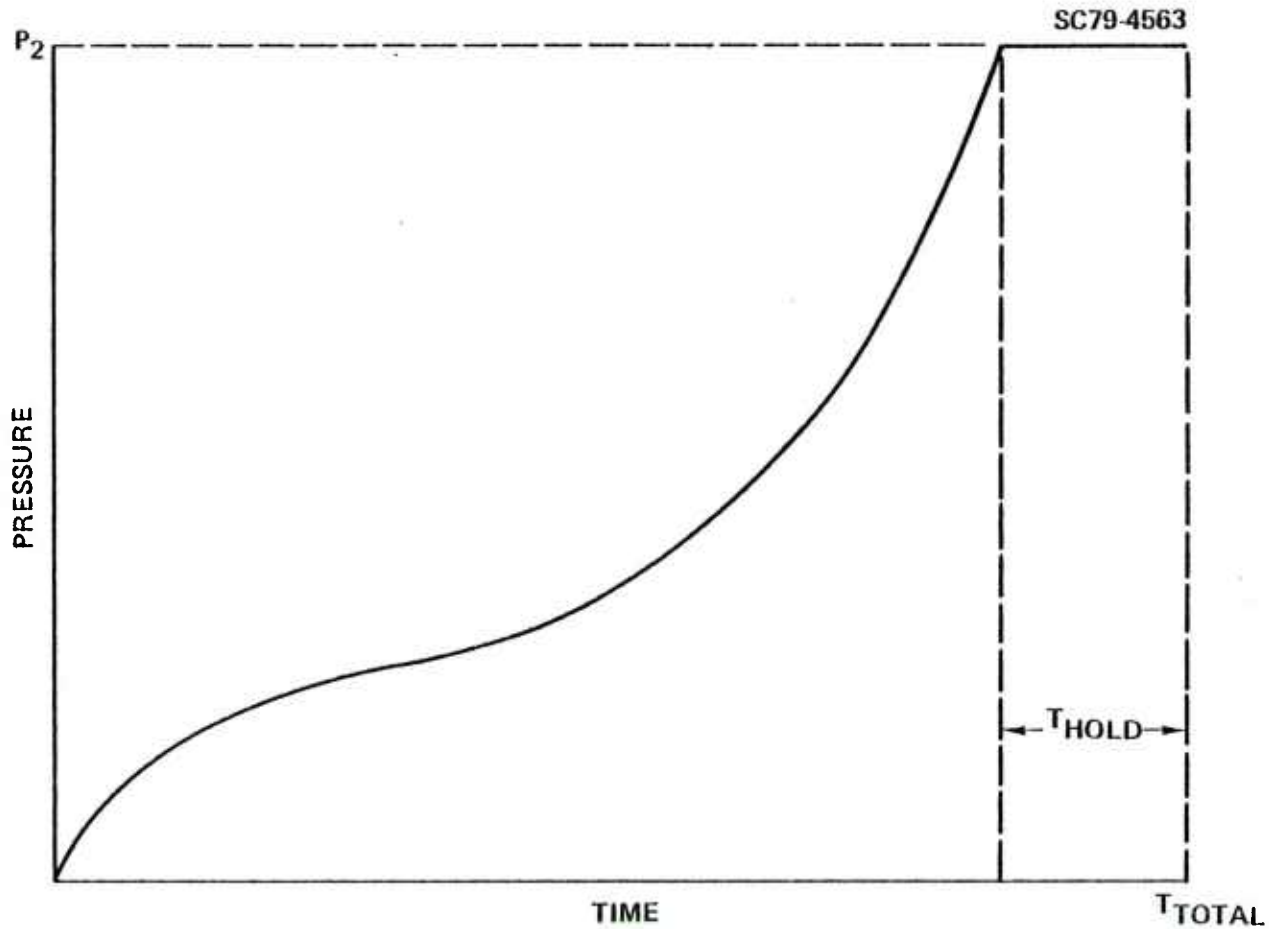

Figure 18. Pressure/time profile for 1.27 cm (1/2 in.) deep superplastically formed test parts. See table 5 for actual pressures used.

5×10^{-3} to 4×10^{-4} s^{-1} and the test temperatures from 482°C (900°F) to 516°C (960°F). The corresponding forming times ranges from just less than 3 min to as high as 51 min.

An example of the part formed which contained the complex configuration is shown in figs. 19 and 20 in which the top and bottom sides of the parts formed are shown. The part shown in figs. 19 and 20 are part no. 7 of table 5 which was formed at a strain-rate of approximately 4×10^{-4} s^{-1}. A second part, part no. 10, was also formed to this configuration with a somewhat higher strain-rate of 10^{-3} s^{-1} and this part was delivered to the Army, ARRADCOM as a demonstration part. Examples of other parts superplastically formed are shown in figs. 21, 22 and 23. The typical part of the 2.54 cm (1 in) deep configuration which was successfully formed is shown in fig. 21. This is part no. 3 outlined in table 5, and was formed at a strain-rate of 4×10^{-4} and a temperature of 516°C (960°F). The part no. 5, shown in fig. 22, ruptured near the die entry radius. The part was formed at 482°C (900°F) and the strain-rate of 10^{-3} s^{-1}. It should be noted that while the strain-rate of 10^{-3} caused rupture of the part no. 5 at 482°C (900°C), forming at that same strain-rate but at the higher temperature of 516°C (960°F) did not cause rupture. An example of a part formed to a more shallow die configuration is shown in fig. 23, which is part no. 8. This was formed at 516°C (960°F) and at a strain-rate of 5×10^{-3} s^{-1}. The resulting die angle at the bottom of the part can be seen to be quite sharp suggesting that rather severe forms can be created in a relatively short time period for this material at 516°C (960°F).

The thinning characteristics were measured for these parts through the mid-section, and an example of the thickness profiles are presented in figs. 24 through 26. For the part no. 1 formed at 516°C (960°F), the thickness profiles are relatively uniform through most areas, except that some thinning appears to be concentrated just below the die entry radius, and is most severe at the higher strain-rate as can be seen for part no. 2, fig. 24. The thinning concentrations appears to be less severe at strain-rates of 4×10^{-4} and 10^{-3} s^{-1} which is consistent with the somewhat higher m values corresponding to those to those latter strain-rates. The thinning profile shown in fig. 25 for the temperature of 482°C (900°F) show substantially

Figure 19. Superplastically formed part no. 7 showing the die contact side of the part.

Figure 20. Superplastically formed part no. 7 showing the inside of the part.

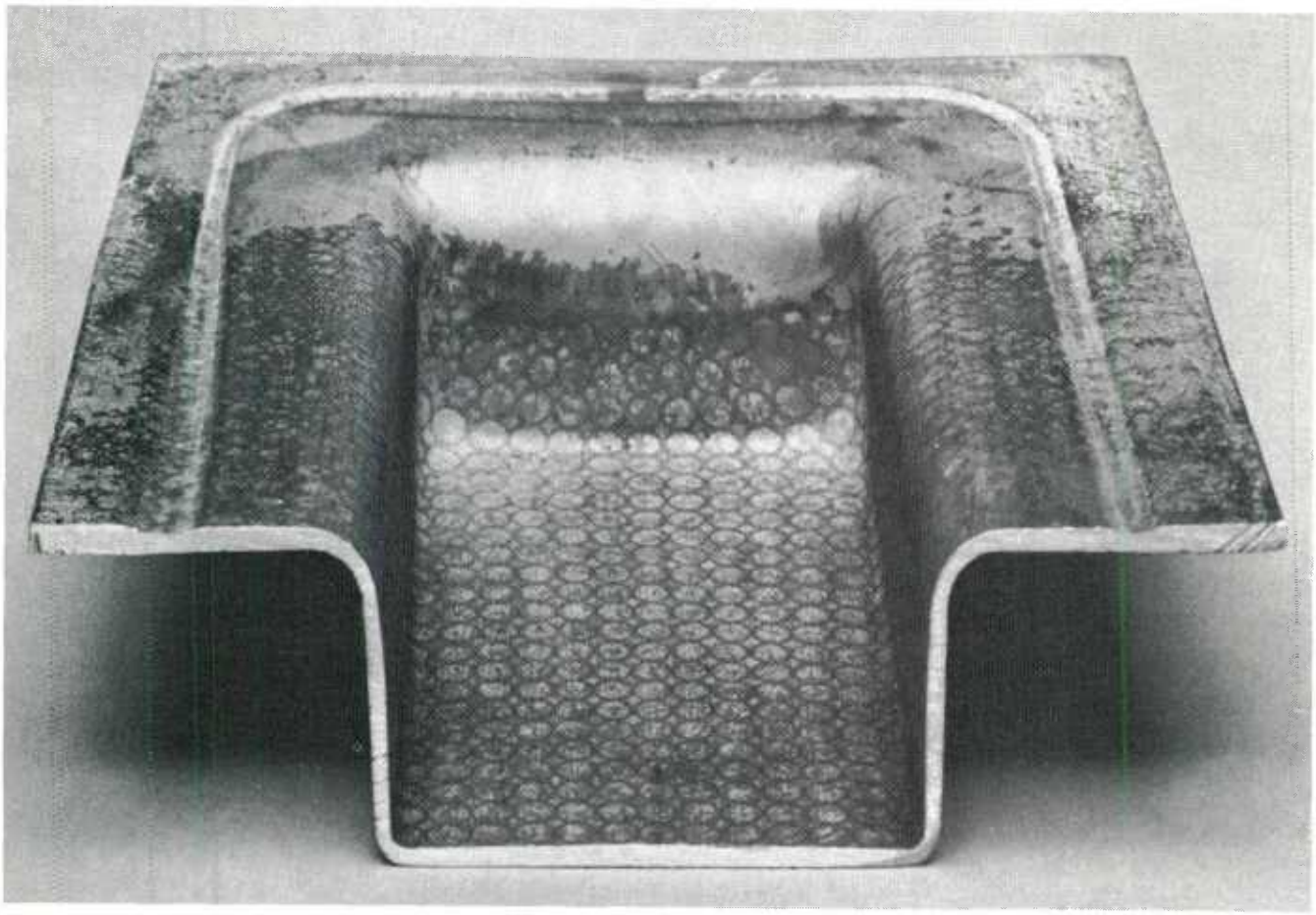

Figure 21. Superplastically formed part no. 3 after cutting in two to facilitate thickness profile measurements.

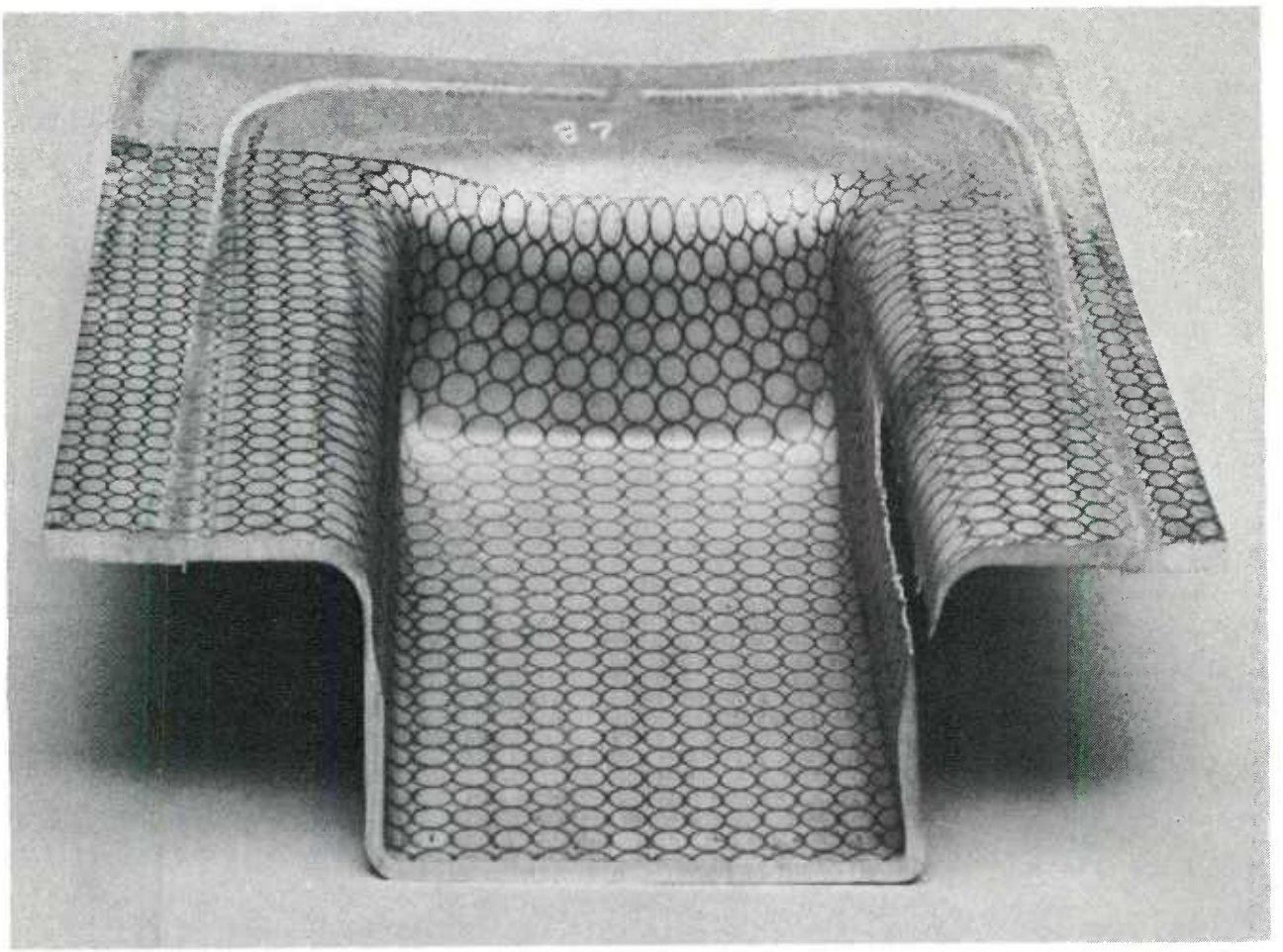

Figure 22. Superplastically formed part no. 5 after cutting in two to facilitate thickness profile measurements. Part ruptured during forming as can be seen on the right hand sidewall of the part.

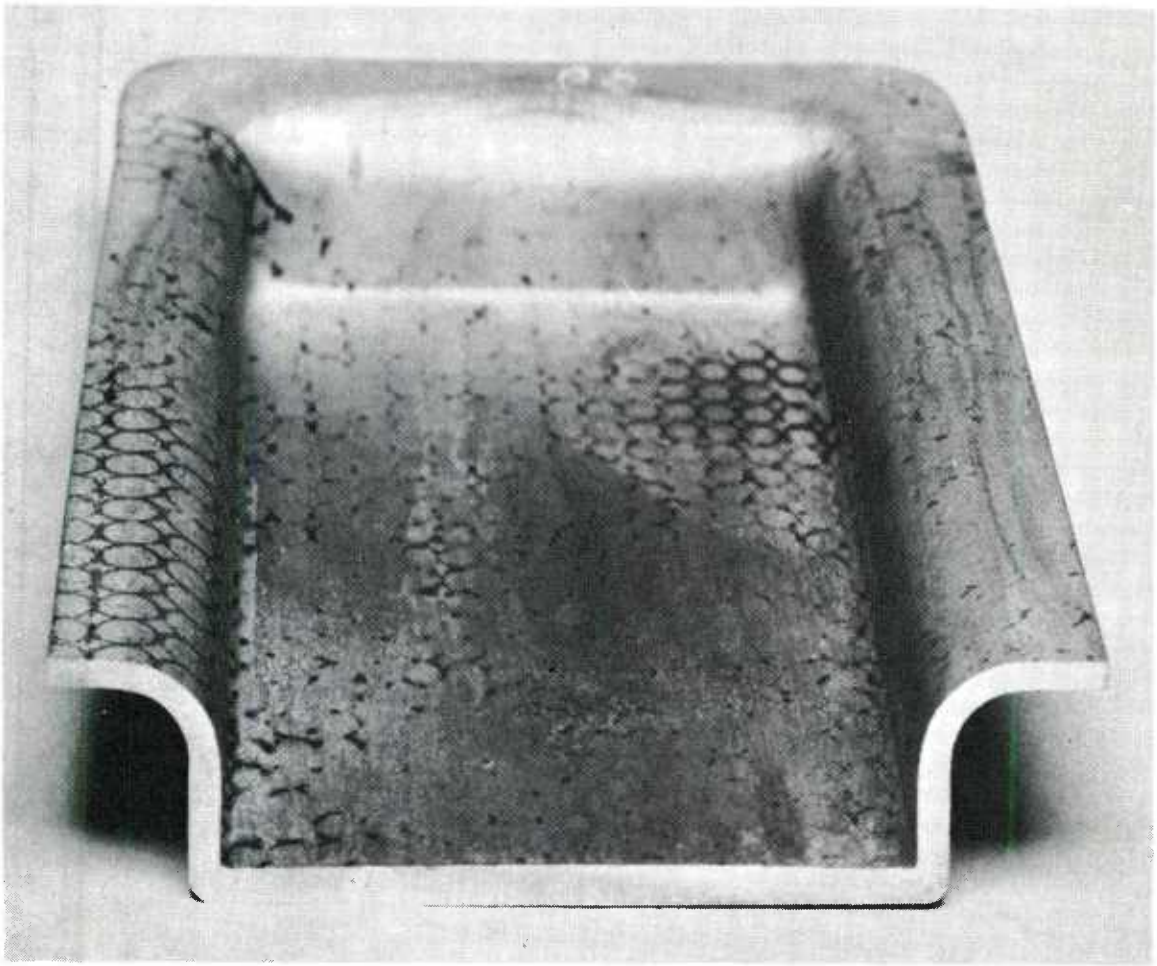

Figure 23. Superplastically formed part no. 8 after being cut in two to facilitate thickness measurements.

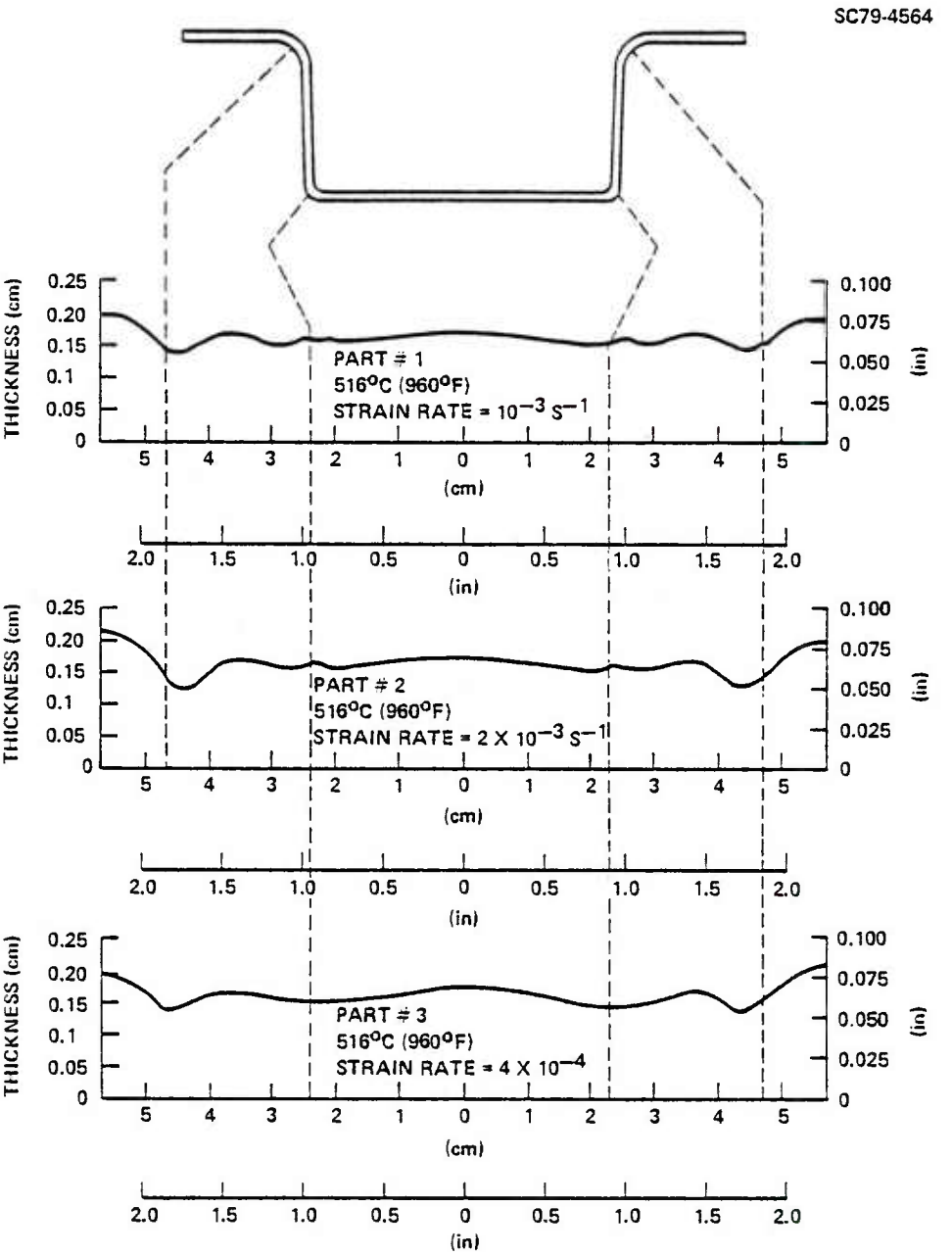

Figure 24. Thickness profiles for superplastically formed parts nos. 1, 2 and 3 which were formed at a temperature of 516°C (960°F).

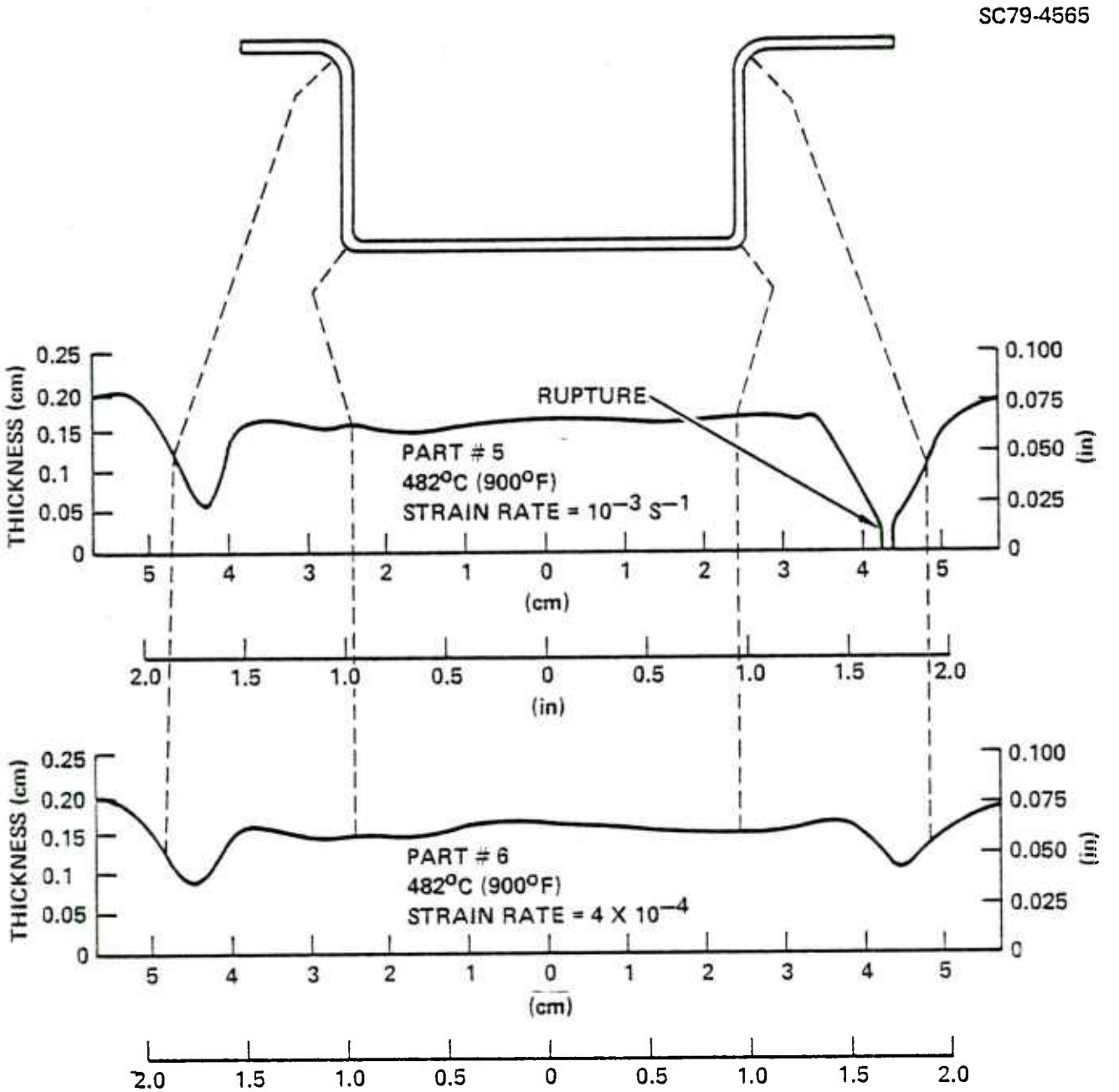

Figure 25. Thickness profiles for parts nos. 5 and 6 formed at 482°C (900°F).

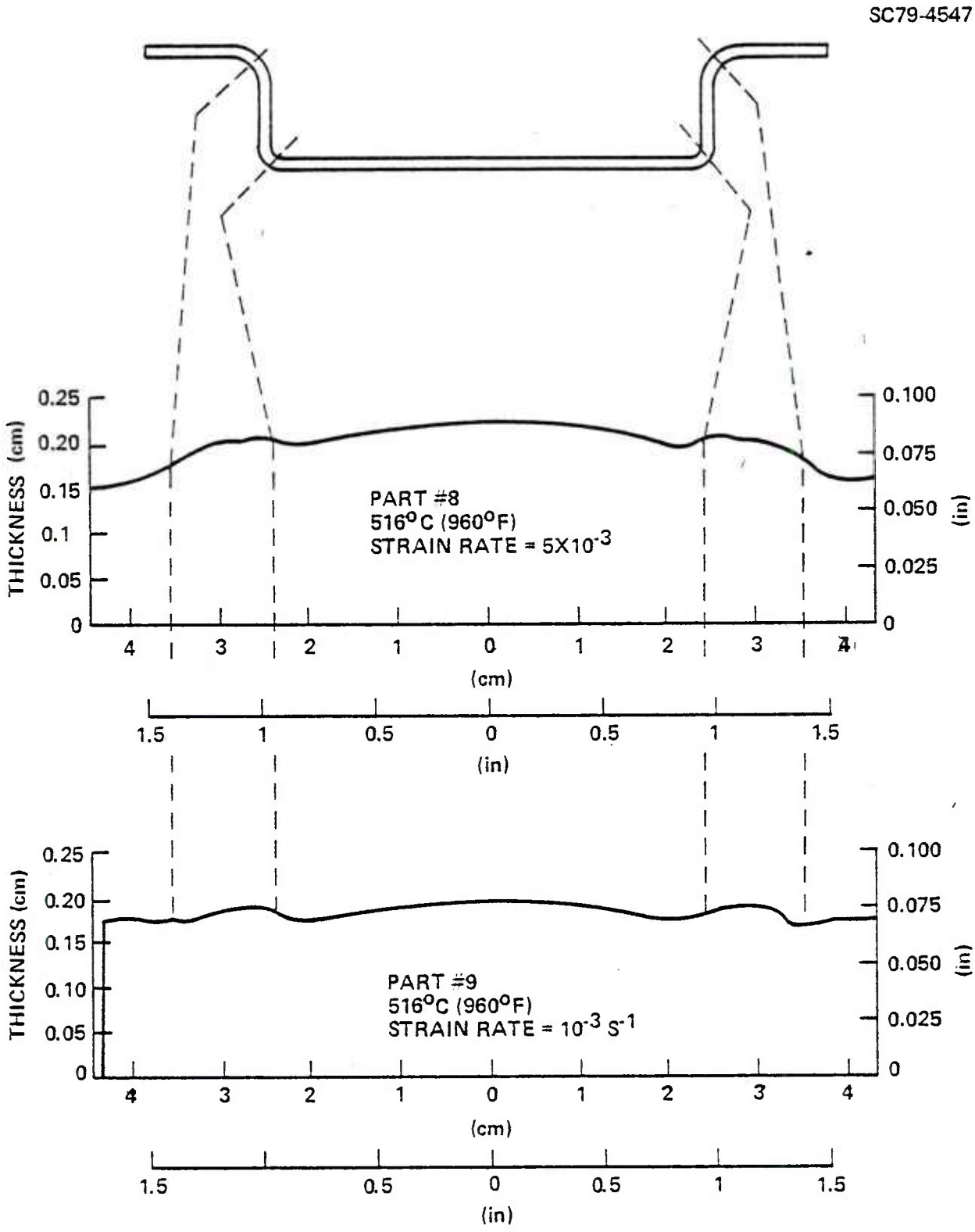

Figure 26. Thickness profiles for parts nos. 8 and 9 which were formed at a temperature of 516°C (960°F).

greater thinning concentration just below the die entry radius. In part no. 5, which was formed at 482°C (900°F) a strain-rate of approximately 10^{-3} s^{-1}, excessive thinning occurred and the part, in fact, ruptured as illustrated in figs. 25 and 22. The thinning through the remainder of the part was quite uniform for both temperatures. For the more shallow part, of 1.27 cm (1/2 in.) deep, the die entry radius does not seem to be excessively thin and the thickness through the part appears to be more uniform than for the deeper configurations.

A number of the superplastically formed aluminum parts were evaluated for microstructural characteristics by optical metallography. Metallographic sections were taken from four key areas of the parts as illustrated in fig. 27. The resulting microstructures are presented in fig. 28, for part no. 1, fig. 29 for part no. 2, and fig. 30 for part no. 3. The microstructures observed in these formed parts are basically in agreement with those microstructures observed in the tensile test specimens in that the grain size stability is apparent and the tendency to form internal cavitation in those areas of large strains is indicated. The most severe cavitation is observed in the corner areas, area 4, where the total strain is the greatest for the parts. It is also observed that the cavitation present appears to be somewhat more severe for the higher strain-rates than for the lower strain-rates of 4×10^{-4} s^{-1}.

DISCUSSION

The results of this program reveal that the technique utilized for refining grain size in the 7475 high strength aluminum alloy was quite effective, and that the grain size developed for this alloy is in the range of 7.5 to 14 μm. This grain size is fine enough to permit the development of a substantial capability for high elongations and superplastic forming utilizing gas pressure (blow forming) techniques. The fine grain size developed in this alloy has been observed to be quite stable at the temperatures evaluated as well as under conditions of deformation over a range of strain-rates. This combination of fine grain size and its stability at elevated temperatures

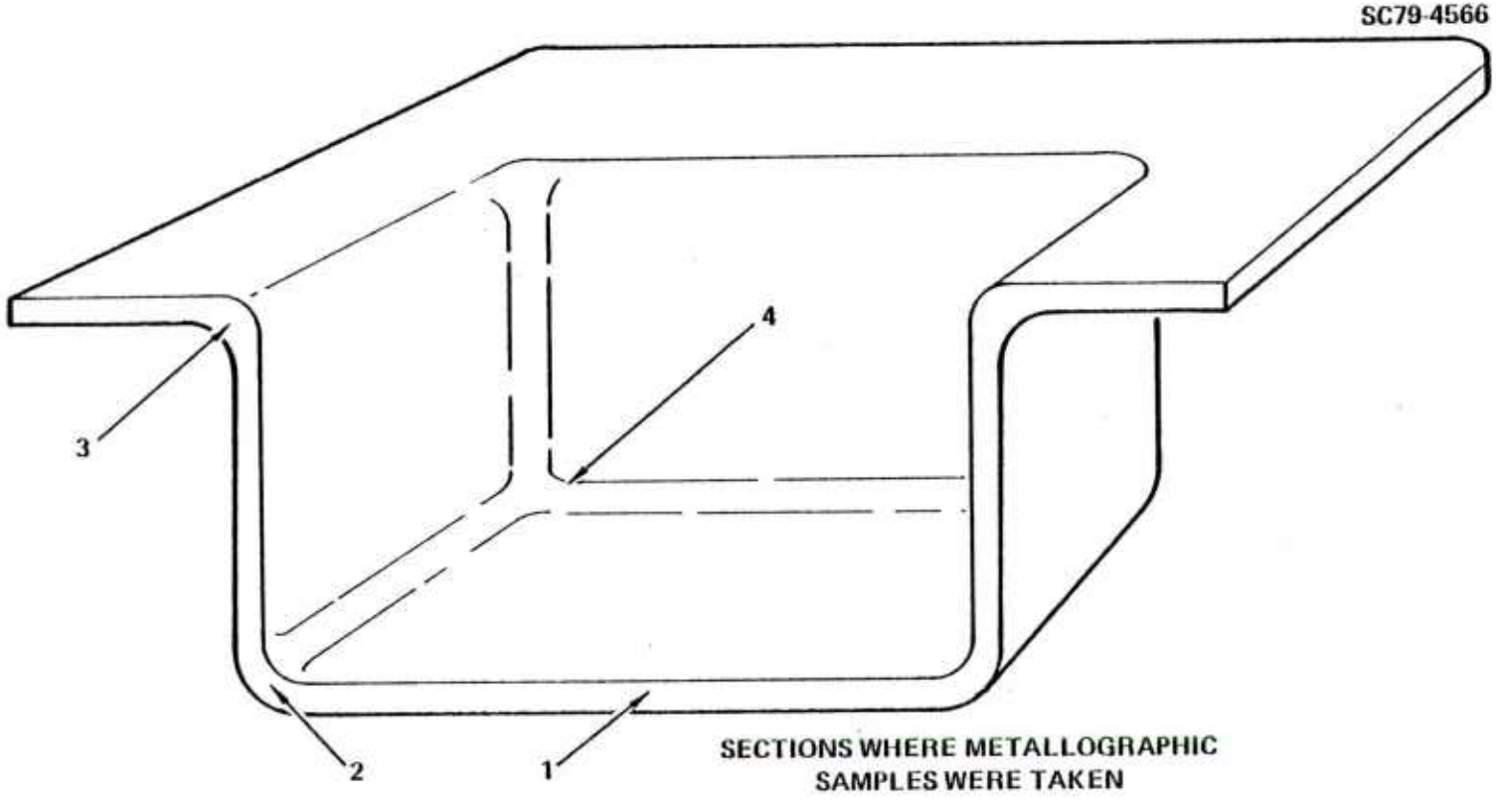

Figure 27. Illustration of a half section of a superplastically formed part showing the locations of metallographic samples presented in figs. 28 through 30.

SC79-4567

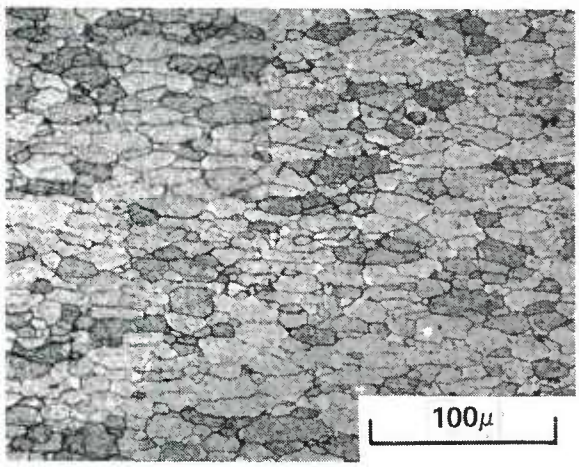

SECTION 1

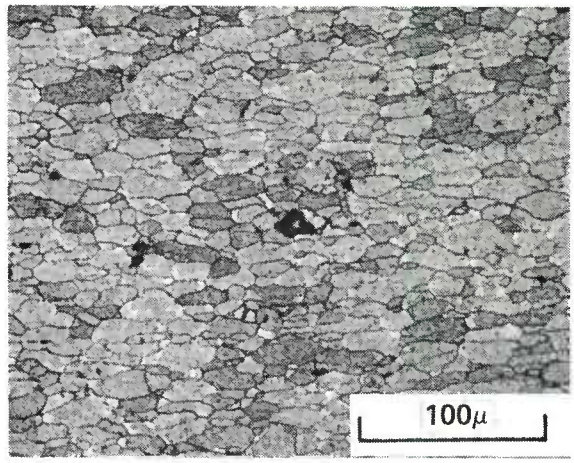

SECTION 2

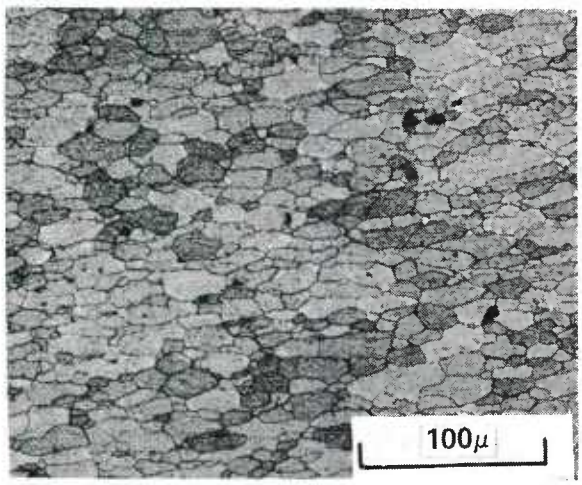

SECTION 3

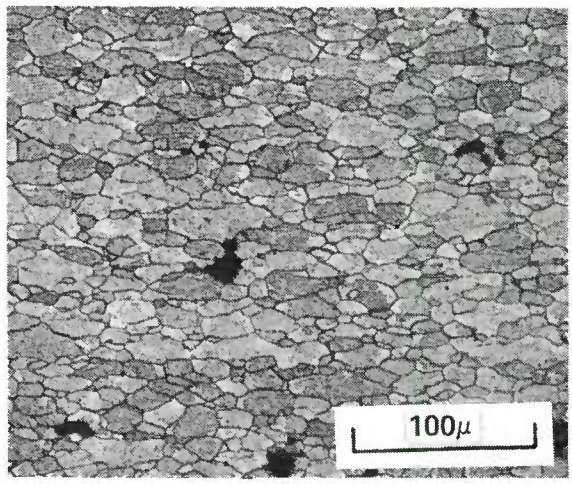

SECTION 4

Figure 28. Optical micrographs of sections taken from four areas of part no. 1. Locations are illustrated in fig. 27.

SC79-4568

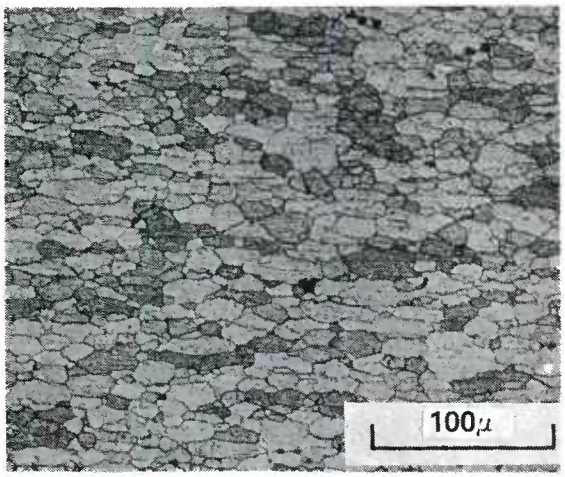

SECTION 1

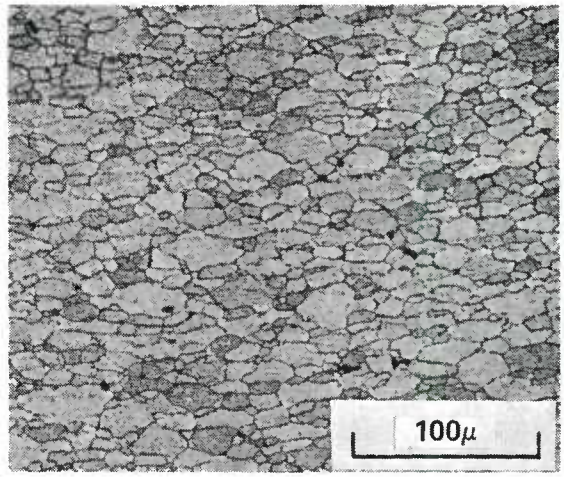

SECTION 2

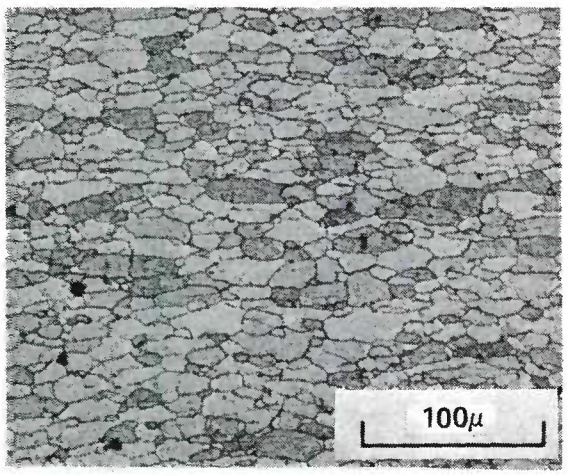

SECTION 3

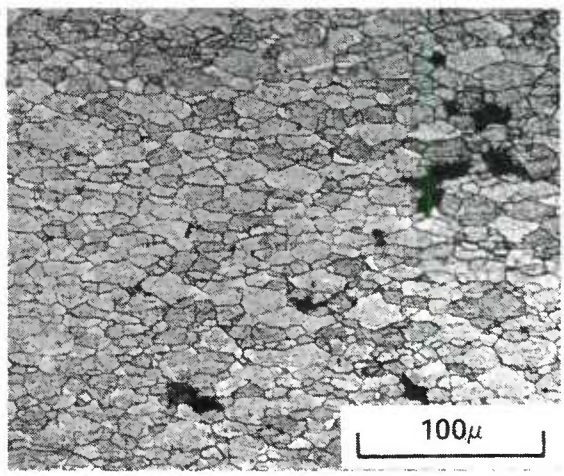

SECTION 4

Figure 29. Optical micrographs of sections taken from four areas of part no. 2. Locations of the sections are illustrated in fig. 27.

SC79-4569

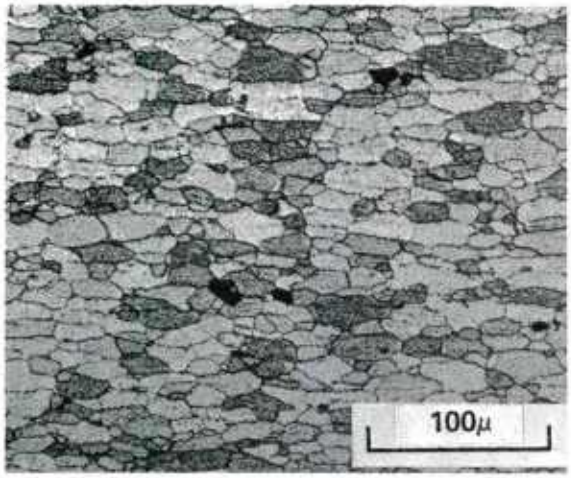

SECTION 1

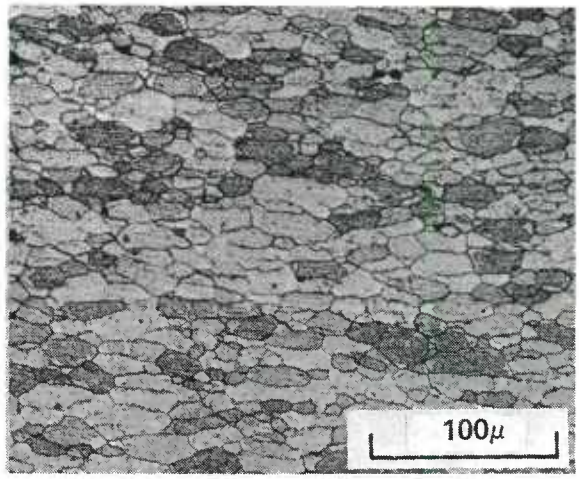

SECTION 2

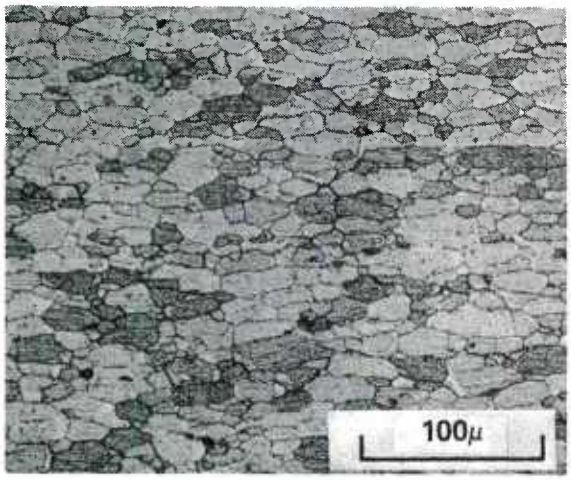

SECTION 3

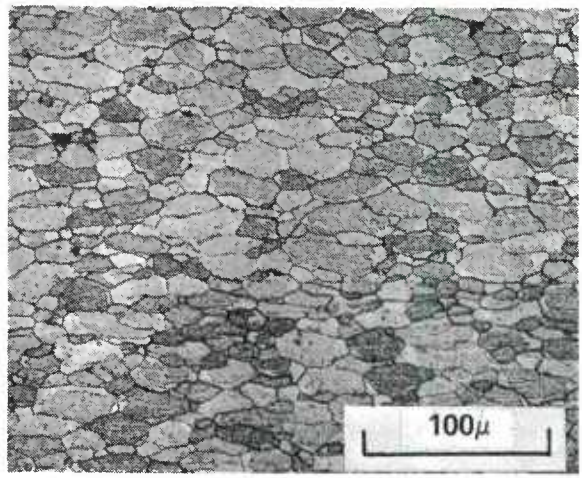

SECTION 4

Figure 30. Optical micrographs of sections taken from four areas of part no. 3. Illustration of the locations of the sections is shown in fig. 27.

permit the achievement of a moderate superplastic capability as demonstrated by tensile elongations in excess of 500%. Corresponding to the high elongations observed, the flow stress of the material is sufficiently low as to permit the use of gas pressure to cause substantial forming. Significant forming can be readily achieved generally using pressures of less than about 4.8 MPa (700 psi) and in most cases forming can be achieved at far lower pressures if the time of forming is extended. The above combination of factors, therefore, suggest that this product has a significant potential for superplastic forming of structural configurations for application to aerospace as well as ground transportation systems.

While the superplastic characteristics of the material were quite good at 516°C (960°F), the slightly lower temperature of 482°C (900°F) results in a much decreased capability for superplastic deformation. The strain-rate sensitivity over a wide strain of strain-rates is much lower for this temperature than for 516°C (960°F) as shown in figs. 5 and 6. The corresponding elongations measured for this alloy at 482°C (900°F) are much lower than for the higher temperature as shown in table 3. The highest elongations for this lower temperature are in the range of 300%, down considerably from a maximum of 650% observed for the higher temperature. The results of the 482°C (900°F) testing of this material are comparable to prior observations of 7075 and 7050 alloy (Ref. 16). It therefore appears that the capability of this material to be processed at a higher temperature is instrumental in achieving the high tensile elongations observed and the high degree of superplasticity indicated through the associated tensile testing. The maximum temperature of exposure for an alloy such as 7075 is approximately 482°C (900°F) because of the tendency to develop incipient melting on exposure to higher temperatures which results in impaired properties of the material. On the other hand, the 7475 aluminum alloy because of the more restricted alloy composition ranges can be processed at a higher temperature of 516°C (960°F) providing, therefore, the opportunity of achieving the high tensile elongations not observed in some of the other 7000 series alloys of comparable grain size.

The potential for forming this alloy into complex configurations utilizing relatively low pressure gas was clearly demonstrated as shown in figs. 19

and 20. Although these parts are of small scale in terms of absolute dimension the severity of forming is substantial and they therefore are considered tc be representative of the unique capability of these materials for superplastic forming. The material, the technique, and the equipment utilized are considered to be adaptable to much larger scale components. Since the parts formed are totally stretch formed, the potential for producing parts of multiple deep drawn sections (as shown in fig. 19) is considered to be well within the capabilities for this material formed by the superplastic forming process. As with any superplastic metal, extensive forming causes noticeable thining in the areas formed (3). The thinning characteristics, however, are consistent with those observations of other materials. The tendency to thin over the die entry radius as shown in fig. 24 can be manipulated by controlling the average strain-rate with which the part is formed. For example, in fig. 24 the most excessive thinning of the die entry radius was observed for part no. 2 formed at a fairly high strain-rate of 2×10^{-3} s^{-1}. However, by reducing the rate of forming of this part to a strain-rate of 4×10^{-4} part no. 3 showed noticeably less thinning in this die entry radius. This variation of thinning is found to follow the trend of the strain-rate sensitivity, m, which is higher for the lower strain-rate than for the higher strain-rate, thus providing greater resistance of the material to developing the local necking over the die entry radius at the lower strain-rate. This characteristic has also been observed for titanium Ti-6Al-4V (ref. 3).

An interesting characteristic of this material is its ability to be very rapidly formed to somewhat modest extents in terms of the superplastic forming characteristics as shown in fig. 23. This part was formed in just less than 3 minutes, which is a fairly rapid process in terms of superplastic forming. However, the part is totally stretch formed and, therefore, the forming capability required to make such a part by this technique is significant and the very sharp radius at the lower edge of the part exceeds the capability available by conventional forming methods. It therefore appears that there may be a number of parts of modest complexity which could be readily formed by this process in very short times, thus providing a forming capability much in excess of conventional forming, but not requiring the full capability of the

superplastic process, i.e., the capability to form very high tensile elongations.

One undesirable characteristic observed for this material is the tendency tc cavitate, or form internal pores during deformation at high temperatures and particularly at high strain levels. Such cavitation is not uncommon to superplastic materials and has been observed in other superplastic aluminum alloys as well as in copper-base, nickel-base and iron-base alloys formed at elevated temperatures under superplastic conditions. The need for further work is indicated in order to provide a thorough characterization of the conditions under which cavitation occurs, the kinetics of the development and its influence on mechanical properties of materials. Other prior work (16) on 7075 fine grain aluminum alloy has shown that the grain size has a pronounced effect on the tendency to cavitate; the finer the grain the less the cavitation. That study also shows that the cavitation of the fine grain aluminum develops slowly, constituting a small fraction of the volume of the material for substantial strains before its growth becomes pronounced and catastrophic ultimately leading to rupture of the material at strains near the total elongation. This would suggest that there is a usable strain range for this material in which cavitation or internal void concentration is at a sufficiently low level as to not create undue complications in the design and complication of the material's structural use. It should be noted at the temperature of 516°C (960°F) and the slower strain-rate of 5×10^{-5} and 2×10^{-4} s^{-1}. The concentration of voids even at high strains does not appear to be substantial as shown in fig. 13.

It appears from the results of this study that the formation of internal voids or cavitation lead ultimately to the linkage of these cavities and fracture or rupture of the material as can be seen in fig. 9. The failures typically observed are similar to those of fig. 9 in that the material does not neck down to a chisel point but rather fractures prior to this failure by a plastic instability. The resistance of the material to necking as shown in fig. 9 is consistent with the high m value measured for this alloy under those test conditions. This m value as shown in fig. 11 is approximately 0.75 and appears to be quite constant to substantial strain as shown. Since the

strain-rate sensitivity, m, is a measure of the resistance of the material to local necking, these results then are consistent with the observation of the tensile samples shown in fig. 9, which did not neck down to any great extent during the straining to high strain levels. If cavitation could be eliminated or reduced, it would be expected that, for these m values, the total elongations observed for this alloy would be noticeably higher than the 500-600% reported.

CONCLUSIONS

1. Thermomechanical processing methods can effectively reduce the grain size of the 7475 Al alloy to the range of 8 to 14 μm.

2. Fine grain sizes of the order of 8 to 14 μm in 7475 Al alloy increase only modestly on exposure to elevated temperatures growing to only about 10 to 20 μm after 24 hours at 516°C (960°F).

3. Grain sizes in the range of 8 to 14 μm in the 7475 Al alloy are sufficiently small and stable to permit the development of superplastic deformations. Tensile elongations of as high as 650% were measured for this material at 516°C (960°F) and a strain rate of 2×10^{-4} s^{-1}.

4. The fine grained 7475 Al alloy can be gas pressure superplastically formed into complex shapes requiring significant tensile elongation. The greatest superplastic capability and easiest forming is achieved at 516°C (960°F).

5. The fine grained 7475 Al alloy tends to develop internal voids or cavities at high strains, during high temperature tensile deformation.

REFERENCES

1. C. H. Hamilton, G. W. Stacker, J. A. Mills and H. W. Li, "Superplastic Forming of Titanium Structures" Air Force Materials Laboratory Report, AFML-63-C-5055, April 1975.

2. C. H. Hamilton and G. E. Stacker, "Superplastic Forming of Ti-6Al-4V Beam Frames," Metals Progress, March, 1976, p 34.

3. C. H. Hamilton, "Forming of Superplastic Metals," Proceedings, AIME Symposium on Formability Analysis, Modeling, and Experimentation," Chicago, Ill., edited by S. S. Hecker, A. K. Ghosh, and H. L. Gegel, p 232-258.

4. S. B. Agrawal, and E. D. Weisert, "Superplastic Forming/Diffusion Bonding (SPF/DB) Process Capabilities and Limits," Air Force Contract F33615-78-C-5016, IR-780-7(IV), Interim Report for period Aug. 16, 1978 through Nov. 15, 1978.

5. C. M. Fleming, "Superplastic Forming/Diffusion Bonding (SPF/DB) Process Limits," Air Force Contract F33615-77-C-5208, Report IR-862-7-IV, Interim Report for the period 16 Aug. through 15 Nov. 1978.

6. E. Di Russo, M. Conserva, M. Buratti, and F. Gatto, "A New Thermomechanical Procedure for Improving the Ductility and Toughness of Al-Zn-Mg-Cu Alloys in the Transverse Directions," Materials Science and Engineering, Vol. 14, p 23-36, 1974.

7. E. Di Russo, M. Conserva, F. Gatto, and H. Markus, "Thermomechanical Treatments on High Strength Al-Zn-Mg (Cr) Alloys," Met. Trans. Vol. 4, p 1133-1144, Apr. 1973.

8. J. Waldman, H. V. Sulinski, and H. Markus, "The Effect of Ingot Processing Treatments on the Grain Size and Properties of Al Alloy 7075," Met. Trans. Vol. 5, p 573-584, Mar. 1974.

9. J. Waldman, H. V. Sulinski, and H. Markus, "New Processing Techniques for Aluminum Alloys," Solidification Technology, Proceedings of the First Army Materials Technology Conference, Portsmouth, New Hampshire, Oct. 22-25, 1972.

10. J. Waldman, H. V. Sulinski, and H. Markus, "Thermomechanical Processing of Aluminum Alloy Ingots," Report No. FA-TA-75052, Frankford Arsenal, Phila., Pa., Aug. 1975.

11. J. Waldman, H. V. Sulinski, and H. Markus, "Processes for the Fabrication of 7000 Series Aluminum Alloys," U.S. Patent 3,847,681, Nov. 12, 1974.

12. N. E. Paton and C. H. Hamilton, "Method of Imparting a Fine Grain Structure to Aluminum Alloys Having Precipitating Constituents," U.S. Patent 4,092,181, April 25, 1977.

13. N. E. Paton, and C. H. Hamilton, "Development of Fine Grain Size in Precipitation Hardenable Aluminum Alloys," to be submitted to Met. Trans.

14. D. Lee and W. A. Backofen, "Superplasticity in Some Titanium and Zirconium Alloys," Trans. TMS-AIME, Vol. 239, p 1034, 1967.

15. A. K. Ghosh and C. H. Hamilton, "Mechanical Behavior and Hardening Characteristics of a Superplastic Ti-6Al-4V Alloy," Met Trans. A, Vol. 10, p. 699-706, 1979.

16. A. K. Ghosh and C. H. Hamilton, "Deformation and Fracture in Aluminum-Zinc-Magnesium Alloys at Elevated Temperatures," Proceedings, 5th International Conference on Strength of Metals and Alloys," Aachem, West Germany, August 27-31, 1979.

Table 1. Composition of 7475 Alloy (%)

Zn	Mg	Cu	Fe	Si	Mn	Cr	Ti
5.2-6.2	1.9-2.6	1.2-1.9	0.12 max	0.10 max	0.06 max	0.18-0.25	0.06 max

Table 2. Results of grain growth measurements for 7475 Al in the temperature range of 477°C (800°F) to 516°C (960°F)

Temperature (°C/°F)	Time (hr)	Grain Intercept Distance (μm)	
		Longitudinal	Short Transverse
516/960	0.25	17.6	8.8
	1	16.9	9.0
	4	18.2	9.2
	8	18.7	9.8
	24	19.0	10.0
493/920	0.25	14.5	7.8
	1	15.3	8.5
	4	16.5	9.1
	8	16.7	9.1
	24	18.3	9.3
482/900	0.25	14.0	7.8
	1	16.5	8.3
	4	16.9	8.4
	8	17.3	8.6
	24	18.2	9.2
454/850	0.25	14.7	7.9
	1	15.7	8.0
	4	16.0	8.0
	8	16.1	8.3
	24	16.5	8.5
427/800	0.25	14.7	7.5
	1	15.7	7.7
	4	15.2	8.1
	8	15.1	7.7
	24	15.0	8.1

Table 3. Results of total elongation tests conducted under constant strain rate conditions

Specimen Orientation	Test Temp. (°C/°F)	Strain Rate (s^{-1})	Total Elongation (%)
L	516/960	10^{-2}	118
LT		10^{-2}	100
L		5×10^{-3}	200
LT		5×10^{-3}	175
L		10^{-3}	275
LT		10^{-3}	>450
L		2×10^{-4}	650
LT		2×10^{-4}	525
L		5×10^{-5}	425
L	482/900	10^{-2}	150
LT		10^{-2}	100
L		5×10^{-3}	125
LT		5×10^{-3}	200
L		10^{-3}	200
LT		10^{-3}	175
L		2×10^{-4}	306
LT		2×10^{-4}	200

L - Longitudinal
LT - Long Transverse

Table 4. Grain size data for tensile specimens

Spec. No.	Temp (°C/°F)	Strain Rate (s^{-1})	Axial Strain (at Location of micro's)	Time at Temp. (min)	Grain Size Observed (μm)		Grain Size Anticipated (μm)(*)	
					Long	S. Trans.	Long	S. Trans.
14L	516/960	5×10^{-3}	1.04	13	10.9	6.9	16.5	8.5
6L		10^{-3}	1.39	32	12.9	9.5	17.0	8.8
16L		2×10^{-4}	1.77	178	15.8	11.6	17.8	9.2
17L		5×10^{-5}	1.77	490	16.3	12.2	18.7	9.8
9L	482/900	5×10^{-3}	.69	12.2	13	7.1	15.4	7.9
1L		10^{-3}	1.09	48	11.4	6.5	15.9	8.1
12L		2×10^{-4}	1.43	126	13	10.1	16.4	8.2

(*) From figure 1.

Table 5. Forming parameters for 7475 superplastic forming demonstration parts

Part No.	Depth (cm/in)	Config.	Forming Temp. (°C/°F)	Strain Rate (s^{-1})	Forming Pressure[a]		Forming Time(min)[a]		
					P_1(MPa/Psi)	(P_2(MPa/Psi)	T_{Total}	T_{Hold}	Comment
1	2.54(1)	Flat Bottom	516/960	10^{-3}	0.36/(52)	1.68/(243	22	2	
2	2.54(1)	Flat Bottom	516/960	2×10^{-3}	0.15/(89)	2.76(400)	12	2	
3	2.54(1)	Flat Bottom	516/960	4×10^{-4}	0.15/(22)	0.69/(100)	80	29	
4	2.54(1)	Flat Bottom	516/960	1×10^{-3}	1.15/(167)	3.06/(444)	22	0	
5	2.54(1)	Flat Bottom	482/900	1×10^{-3}	0.91/(133)	4.83/(700)	30	Part ruptured	
6	2.54(1)	Flat Bottom	482/900	4×10^{-4}	0.57/(83)	2.76(400)	60	9	
7	2.54(1)	Bead + Step	516/960	4×10^{-4}	0.15(22)	0.69(100)	80	29	
8	1.27(1/2)	Flat Bottom	516/960	5×10^{-3}	(b)	6.90/(1000)	3.35	.5	
9	1.27(1/2)	Flat Bottom	516/960	10^{-3}	(b)	2.85/(413)	22.5	7.5	
10	2.54(1)	Bead + Step	516/960	10^{-3}	0.35(52)	2.07/(300)	29	Delivered to ARRADCOM	

(a) See figs. 17 and 18 for description of pressure and time parameters.
(b) No plateau in pressure for this configuration (see fig. 18).

DISTRIBUTION LIST

Director
Defense Research and Engineering Office
ATTN: DDRE (R&AT)
Washington, DC 20310

Director
Defense Advanced Research Projects Agency
ATTN: Dr. E. Van Reuth
1400 Wilson Boulevard
Arlington, VA 22209

Administrator
Defense Technical Information
ATTN: Accessions Division (DDC-TC) (12)
Cameron Station
Alexandria, VA 22314

Assistant Secretary of the Army (R&D)
ATTN: Deputy for Science and Technology
Washington, DC 20310

Deputy Chief of Staff for Research, Development and Acquisition
Department of the Army
ATTN: DAMA-ARZ-D
Washington, DC 20310

Commander
US Army Armament Research and Development Command
ATTN: DRDAR SC, Col. A. J. Larkins
DRDAR-SCM-P, Dr. Waldman (7)
DRDAR-SCP
DRDAR-TSS (5)
Dover, NJ 07801

Commander
US Army Materiel Development and Readiness Command
ATTN: DRCMT, Mr. L. Croan
5001 Eisenhower Avenue
Alexandria, VA 22333

Commander
US Army Materials and Mechanics Research Center
ATTN: DRXMR, Dr. E. Wright
Watertown, MA 02172

Commander
US Army Tank Automotive Research and Development Command
ATTN: DRDTA-RKA, Mr. V. Pagano
Warren, MI 48090

Commander
US Army Aviation Research and Development Command
ATTN: DRDAV-EXT, Mr. G. Gorline
PO Box 209
St. Louis, MO 63166

Director
US Army Mobility Equipment Research and Development Command
ATTN: DRDME-MMM, Mr. E. York
Fort Belvoir, VA 22060

Director
US Army Advanced Materials Concept Agency
ATTN: Technical Information Division
2471 Eisenhower Avenue
Alexandria, VA 22314

Director
US Army Industrial Base Engineering Activity
ATTN: DRXIB-MT, Mr. G. Ney
Rock Island, IL 61299

Commander
US Army Research and Standardization Group (Europe)
ATTN: DRXSN-E-RM, Dr. R. Quattrone
PO Box 65
FPO, New York 04510

Commander
US Army Foreign Science and
Technology Center
ATTN: Mr. W. F. Marley
220 Seventh Street, N.E.
Charlottesville, VA 11901

Commander
US Army Research Office
ATTN: Metallurgy & Materials
Science Division,
Dr. G. Mayer, Director
PO Box 12211
Research Triangle Park, NC 17709

Director
Ballistic Research Laboratory
ATTN: DRDAR-BLT, Dr. D. Dietrich
Aberdeen Proving Ground, MD 21010

Commander
Naval Air Systems Command
Department of the Navy
ATTN: AIR 5203, Mr. R. Schmidt
Washington, DC 20361

Commander
US Naval Surface Weapons Center
ATTN: Dr. S. Fishman, R32
White Oak, MD 20910

Commander
US Naval Surface Weapons Center
ATTN: Mr. W. Mannschreck, Code G54
Dahlgren, VA 22448

Commander
Naval Air Development Center
Johnsville
Aero Materials Department
ATTN: Mr. F. Williams
Warminister, PA 18974

Commander
Air Force Flight Dynamics Laboratory
ATTN: AFFDL/FB, Mr. L. Kelly
Wright Patterson Air Force Base
Dayton, OH 45433

Director
Air Force Materials Laboratory
ATTN: AFML/XR, Dr. T. M. F. Ronald
AFML/Technical Library
AFML/LTM, Mr. B. Kosmal
AFML/LLS, Mr. W. Griffith
Dr. L. R. Bidwell
Wright Patterson Air Force Base
Dayton, OH 45433

Director
Air Force Armament Laboratory
ATTN: AFATL/DLOSL
Elgin AFB, FL 32542

Director Aeronautical System
Division
ATTN: ASD/PMD (PESO), Mr. L. Clark
Wright Patterson Air Force Base
Dayton, OH 45433

Director
National Academy of Science
ATTN: Materials Advisory Board
2101 Constitution Avenue, N.W.
Washington, DC 20418

Metals and Ceramic Information
Center
Battelle Memorial Institute
505 King Avenue
Columbus, OH 43201

Weapon System Concept TEAM/CSL
ATTN: DRDAR-ACW
Aberdeen Proving Ground, MD 21010

Director
US Army Ballistic Research
Laboratory
ARRADCOM
ATTN: DRDAR-TSB-S
Aberdeen Proving Ground, MD 21005

Technical Library
ATTN: DRDAR-CLJ-L
Aberdeen Proving Ground, MD 21010

Benet Weapons Laboratory
Technical Library
ATTN: DRDAR-LCB-TL
Watervliet, NY 12189

Commander
US Army Armament Materiel Readiness Command
ATTN: DRSAR-LEP-L
Rock Island, IL 61299

Director
US Army TRADOC Systems Analysis Activity
ATTN: ATAA-SL (Technical Library)
White Sands Missile Range, NM 88002

US Army Materiel Systems Analysis Activity
ATTN: DRXSY-MP
Aberdeen Proving Ground, MD 21005

Project Manager, Advanced Attack Helicopter
ATTN: AMCPM-AAH, TM
PO Box 209
St. Louis, MO 63166

Project Manager
Advanced Scout Helicopter
ATTN: AMSAV-SIA
PO Box 209
St. Louis, MO 63166

Project Manager, Blackhawk
ATTN: AMCPM-UA-T
PO Box 209
St. Louis, MO 63166

Project Manager, CH-47 Modernization
ATTN: AMCPM-CH47M
PO Box 209
St. Louis, MO 63166

Project Manager, Aircraft Survivability Equipment
ATTN: AMCPM-ASE-TM
PO Box 209
St. Louis, MO 63166

Project Manager, Cobra
ATTN: AMCPM-CO-T
PO Box 209
St. Louis, MO 63166

Director
Eustis Directorate
US Army Air Mobility R&D Lab
ATTN: SAVDL-EU-TAS
Ft. Eustis, VA 23604

Director, Ames Directorate
US Army Air Mobility R&D Lab
ATTN: SAVDL-AM
Ames Research Center
Moffett Field, CA 94035

Director, Langley Directorate
US Army Air Mobility R&D Lab
ATTNB: SAVDL-LA
Mail Stop 266
Hampton, VA 23365

Director Lewis Directorate
US Army Air Mobility R&D Lab
ATTN: SAVDL-LE
21000 Brook Park Road
Cleveland, OH 44135

Bell Helicopter Co.
ATTN: Mr. P. Baumgartner, Chief, Manufacturing Technology
PO Box 482
Ft. Worth, TX 76101

Boeing Aerospace Co.
ATTN: D. B. Arnold
PO Box 3999, MS41-37
Seattle, WA 98124

Boeing Vertol Company
ATTN: Mr. R. Pinckney, Mfg. Tech.
Box 16858
Philadelphia, PA 19142

Fairchild Republic Co.
ATTN: Mr. A. Shames
Farmingdale, L.I., NY 11735

FMC Corporation
ATTN: Mr. D. R. Fylling
1105 Coleman Ave. Box 1201
San Jose, CA 95108

General Dynamics Corp.
Confair Aerospace Div.
ATTN: W. Kao
Keraney Mesa Pland
San Diego, CA 02112

Gould Inc., Gould Laboratories
ATTN: Mr. E. L. Thellman
540 E 105th St.
Cleveland, OH 44108

Grumman Aerospace Corp.
ATTN: Dr. P. Adler
Bethpage, NY 11714

Hughes Helicopter
Division of Summa Corp.
ATTN: Mr. R. E. Moore, Bldg. 314
M/S T-419
Centinella Ave. & Teale St.
Culver City, CA 90230

ITT Research Institute
ATTN: Director of Research
10 West 35th St.
Chicago, IL 60616

Inco, Inc.
Inco, R&D Center
ATTN: Dr. J. Benjamin
Sterling Forest
Suffren, NY 10901

Kaiser Aluminum & Chem. Co.
The Center for Technology
ATTN: Mr. L. Barker
PO Box 877
Pleasanton, CA 94566

Kaman Aerospace Corp.
ATTN: Mr. A. S. Falcone
Chief, Materials Engineering
Bloomfield, CT 06002

Lockheed Georgia Co.
D 72-26 Zone 329
ATTN: Dr. Walter Cremens
Marietta, GA 30060

LVT Aerospace
Vought Aeronautics Division
ATTN: Chief, Mat'ls Processes
PO Box 5907
Dallas, TX 75222

McDonnell Douglas Corp.
Douglas Aircraft Co.
3855 Lakewood Blvd.
ATTN: Chief, Materials & Processes
Long Beach, CA 90846

Northrop
Mail Code 3872/62
ATTN: Dr. G. Chanani
3901 W. Broadway
Hawthorne, CA 90250

Rockwell International
North Americal Aircraft Division
ATTN: Chief Mat'ls & Processes
International Airport
Los Angeles, CA 90009

Sikorsky Aircraft Division
United Aircraft Corp.
ATTN: Mr. S. Silverstein
Section Supv., Mfg. Tech.
Stratford, CT 06497

United Technologies Corp.
Pratt & Whitney Aircrafts Div.
Manufacturing Research and
Development
ATTN: Mr. Ray Traynor
East Hartford, CT 06108

Vought Corp.
ATTN: Dr. D. H. Petersen
PO Box 6144
Worcester St.
North Grafton, MA 01536

Wyman-Gordon Co.
ATTN: Mr. M. E. Rand
Worcester St.
North Grafton, MA 01536

Prof. M. C. Flemings
Department of Metallurgy
Materials Science
Massachusetts Institute of
Technology
Cambridge, MA 02139

Mr. H. Y. Hunsicker
Aluminum Co. of America
ALCOA Technical Center
ALCOA Center, PA 15069

Mr. M. V. Hyatt
Organization B-8833
Mail Stop 73-43
The Boeing Company
PO Box 3707
Seattle, WA 98124

Prof. C. Laird
Dept. of Metallurgy and Materials
Science
University fo Pennsylvania
Philadelphia, PA 19174

Mr. P. Mackmeier
Materials Technology
MZ 1860
General Dynamics Corporation
Ft. Worth Division
Ft. Worth, TX 76010

Mr. H. Markus
550 S. Ocean Blvd.
Apt. 204-S
Boca Raton, FL 33432

Mr. R. E. Newcomer
Dept. 247, Bldg. 32
McDonnell Douglas Corporation
PO Box 516
St. Louis, MO 63166

Dr. E. J. Ripling
Materials Research Laboratory, Inc.
No. 1 Science Road
Glenwood, IL 60425

Mr. G. Spangler
Reynolds Metal Company
4th and Canal Streets
Richmond, VA 23219

Professor E. Starke
Fracture and Fatigue Research Lab
Georgia Institute of Technology
Atlanta, GA 30332

Mr. H. C. Turner
Branch Manager, Metallic Materials
Dept. 372, Bldg. 33
McDonnell Douglas Aircraft Corp.
PO Box 516
St. Louis, MO 63166

Mr. G. G. Wald
Dept. 78-40, Bldg. 63, Plant A-1
Lockheed Aircraft Company
PO Box 551
Burbank, CA 91503

Mr. W. Weiss
Boeing Vertol Company
PO Box 16858
M/S P32-38
Philadelphia, PA 19142

Mr. Charles E. Doyle
Mail Zone 2830
General Dynamics
Fort Worth Division
PO Box 748
Forth Worth, Texas 76101

Mr. W. F. Bates
D/72-76
2329
Lockheed Georgia Co.
Marietta, GA 30063